Heliyon 10 (2024) e37788

Contents lists available at ScienceDirect

Heliyon

journal homepage: www.cell.com/heliyon

Research article

Marine plankton community and net primary production responding to island-trapped waves in a stratified oligotrophic ecosystem

Zrinka Ljubešić [a,1], Hrvoje Mihanović [b,*,1], Antonija Matek [a], Maja Mucko [a], Eric P. Achterberg [c], Melissa Omand [d], Branka Pestorić [e], Davor Lučić [f], Hrvoje Čižmek [g], Barbara Čolić [g], Cecilia Balestra [h], Raffaella Casotti [i], Ivica Janeković [j,k], Mirko Orlić [l]

[a] University of Zagreb, Faculty of Science, Department of Biology, Horvatovac 102A, 10000, Zagreb, Croatia
[b] Institute of Oceanography and Fisheries, Šetalište I. Meštrovića 63, 21000, Split, Croatia
[c] GEOMAR Helmholtz Centre for Ocean Research, Kiel Wischhofstraβe 1-3, D-24148, Kiel, Germany
[d] University of Rhode Island, Graduate School of Oceanography, 215 South Ferry Rd, Narragansett, RI, 02882, USA
[e] University of Montenegro, Institute of Marine Biology, Put I Bokeljske brigade 68, 85330, Kotor, Montenegro
[f] University of Dubrovnik, Institute for Marine and Coastal Research, Kneza Damjana Jude 12, 20000 Dubrovnik, Croatia
[g] Marine Explorers Society 20.000 leagues, Put Bokanjca 26A, 23000, Zadar, Croatia
[h] National Institute of Oceanography and Applied Geophysics – OGS, Borgo Grotta Gigante 42/C, 34010 Sgonico (TS), Italy
[i] Department of Integrative Marine Ecology, Stazione Zoologica Anton Dohrn, Villa Comunale, 80121, Naples, Italy
[j] Ocean Graduate School and the UWA Oceans Institute, The University of Western Australia, Cnr Fairway and Service Road 4, M470, Crawley, WA, 6009, Australia
[k] GEKOM (Geophysical and Ecological Modelling) Ltd, Fallerovo šetalište 22, 10000, Zagreb, Croatia
[l] University of Zagreb, Faculty of Science, Department of Geophysics, Horvatovac 95, 10000, Zagreb, Croatia

ARTICLE INFO

Keywords:
Internal wave
Biophysical coupling
Adaptive sampling
Plankton diversity
Zooplankton-associated bacteria
Adriatic Sea

ABSTRACT

The oligotrophic Adriatic Sea is characterized during a typical summer by low productivity caused by strong water column stratification, which inhibits vertical mixing and nutrient supply to the euphotic zone. These conditions can be disrupted by transient physical forcing, which enhances nutrient fluxes and creates localized hotspots of relatively high net primary production. In this study, plankton abundance and diversity were investigated in relation to the physical forcing and nutrient concentrations in an area affected by island-trapped waves (ITWs) near Lastovo Island (Adriatic Sea). The episodic ITW events resulted in enhanced uplift and vertical excursion of the thermocline, marked by anomalously higher nutrient concentrations and a corresponding increase in net primary production in the thermocline layer. Physicochemical properties explained 11.7 % ($p = 0.002$) of the variability in micro- and nanophytoplankton and 88.9 % ($p = 0.001$) in the picoplankton community. A significant response to the ITW phenomenon in the plankton community composition ($p = 0.001$) was observed for bacterioplankton. Among the identified amplicon sequence variances, primary producers were scarce and mainly represented cyanobacteria (*Synechococcus* strain CC9902), stramenopiles (*Pelagomonas*), and chlorophytes (*Ostreococcus*). The remaining amplicon sequence variances were assigned to the classes Copepoda, parasitic fungi (*Meyerozyma* spp.), mixotrophic dinoflagellates (family Peridiniales, mostly the genus *Blastodinium*), and parasitic Ciliophora (*Scuticociliata*). Bacterial

* Corresponding author.
E-mail address: hrvoje.mihanovic@izor.hr (H. Mihanović).
[1] Equal contribution.

https://doi.org/10.1016/j.heliyon.2024.e37788
Received 20 January 2024; Received in revised form 31 August 2024; Accepted 10 September 2024
Available online 11 September 2024

ecological functions corresponded to chemoheterotrophic, degradation, and fermentation processes, whereas samples collected after the most intense ITW episode also showed abundant bacteria linked to microplastic degradation and parasitosis. These results highlight the ecological role of localized physical phenomena in enhancing nearshore primary productivity and fine shifts in plankton taxa in oligotrophic systems.

1. Introduction

Primary production provides the basis for life on Earth and marine phytoplankton are key players responsible for approximately half of biologically mediated carbon fixation [1,2]. Net primary production (NPP) is characterized by high spatial and temporal patchiness resulting from interactions between physicochemical and biological processes [1]. As ocean temperatures rise due to climate change, water column conditions are becoming more stratified. Therefore, it is highly important to observe and model the pathways of nutrient fluxes to the euphotic layer and recognize the role of episodic events in creating hotspots for enhanced NPP. The

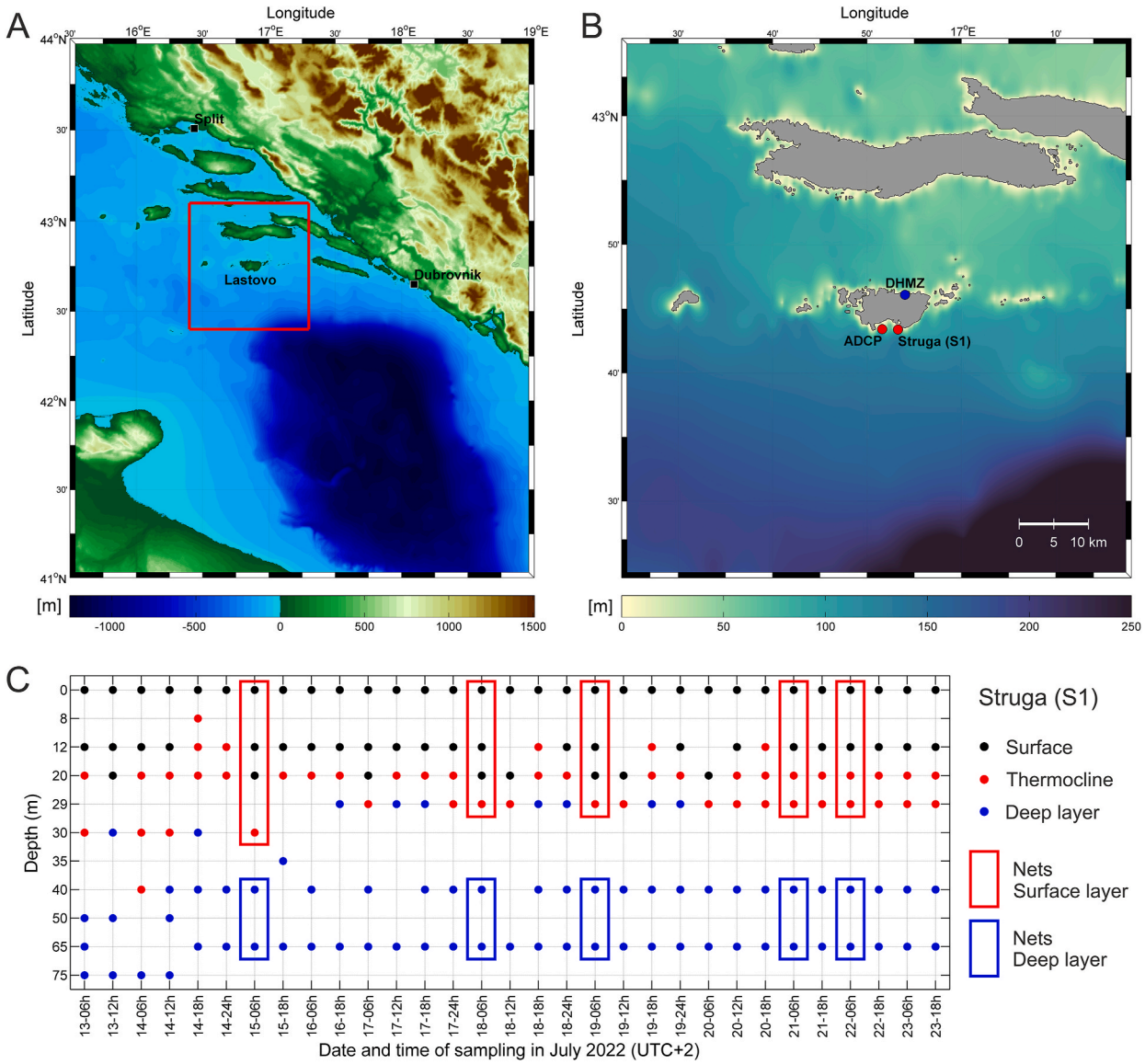

Fig. 1. (A) Study area (Lastovo Island, South Adriatic Sea), (B) sampling stations for ADCP and Struga site (S1), superimposed on a bathymetric map, and (C) timing and depths of discrete sample collection during the 2022 experiment. Lastovo meteorological station (DHMZ) is indicated in (B).

latter is frequent but underappreciated in regions with upwelling or enhanced diapycnal mixing. Increased NPP around small islands has been observed, known as the Island Mass Effect (IME) [3]. The global importance of the small-scale physical and biogeochemical processes of the IME has been documented and the complexity of the physical processes responsible for increased nutrient inputs into the euphotic layer and the uniqueness of each island have been reported [4,5].

Regions influenced by internal island-trapped waves (ITWs), a special case of coastal-trapped waves (CTWs) [6], have been reported as productivity hotspots. Internal ITWs have been observed globally around a small number of islands, including Bermuda in the central Atlantic Ocean [6,7], Hawaii in the central Pacific [8–10], Gotland in the Baltic Sea [11], Mallorca Island in the western Mediterranean [12], Lastovo Island in the Adriatic Sea [13,14], and the Saint Pierre and Miquelon archipelago in the northwestern Atlantic Ocean [15]. Thermocline oscillations at Lastovo Island are driven by diurnal tides and wind forcing (sea and land breezes). Various studies between 2001 and 2011 have investigated the physical forcing around Lastovo Island and discovered that the most pronounced thermocline oscillations at Lastovo (ranging up to 30 m) were due to diurnal winds [14], while barotropic tidal flow produced less intense but more prolonged ITWs [13,16,17]. The physical mechanism driving diurnal temperature oscillations remained elusive for some time. Novosel et al. [16] and Mihanović et al. [17] hypothesized that the interaction of barotropic diurnal tides with the steep shelf break in the South Adriatic resulted in diurnal vertical fluctuations of the pycnocline. However, diurnal tides at latitudes greater than ~30° are subinertial, and diurnal internal tides there can only exist as waves trapped at the shelf break [18]. Subsequently, Mihanović et al. [13] reported that the island bathymetry itself interacts through resonance with the diurnal barotropic tidal flow, and generates large thermocline oscillations around the island. In addition, Orlić et al. [14] showed that wind-driven resonant ITW episodes at Lastovo are even more pronounced. Finally, it was hypothesized that thermocline oscillations could be a driver of nutrient fluxes and diurnal variations in the deep chlorophyll *a* maximum (from 30 to 70 m depth) [19].

The South Adriatic Sea is the least productive part of the Adriatic [20–22]. Interannual variations in primary production in the Middle and South Adriatic Sea are driven by circulation dynamics [23,24] and primary productivity may be increased locally, for example at Palagruža Sill, where nutrients are brought to the surface layer due to upwelling caused by the enhanced inflow of Mediterranean waters [20,25]. Owing to oligotrophy, the most significant primary producers in the Adriatic Sea are fast-adapting and actively dividing pico-sized organisms [19,26,27].

This study aims to demonstrate the linkages between island-trapped waves and NPP in the unique environment around Lastovo Island. The objectives of this study were to (i) detect ITW episodes in available temperature time series and meteo-oceanographic data; (ii) identify the possible impacts of ITW events on NPP and plankton communities; and (iii) elucidate the functional ecological roles of bacterioplankton before, during, and after an ITW event.

2. Materials and methods

2.1. Sampling design

During the water column stratification period in 2021 and 2022, a set of thermistors (HOBO Pendant Temperature/Light 64K Data Logger) was deployed at nine equidistant depths between 5 and 45 m (measurements interval was 5 min) at rocky cliffs in the south of Lastovo Island (Station Struga; S1; Fig. 1; latitude: 42° 43.40′ N, longitude: 16° 53.27′ E). At the same time, an ADCP (RDI WorkHorse 300 kHz) moored at a location to the west of Struga station recorded currents at 4 m depth intervals, with 10 min temporal resolution (Fig. 1; latitude: 42° 43.42′ N, longitude: 16° 51.61’ E). Current measurements during 2021 encompassed depths between 11.0 and 83.0 m, while in 2022 the instrument was deployed nearby in a slightly deeper area, resulting in vertical coverage from 9.5 to 85.5 m.

Ship-based surveys were conducted at S1 station in July of 2021 and 2022. In 2021, profiles for temperature, salinity, chlorophyll *a* fluorescence, and oxygen (T-S-Chl F-Oxygen) were measured twice a day using a CTD probe (SBE 19, Sea-Bird Electronics Inc., USA) with 0.5 m depth averaging. The first measurement was at approximately 06:00 h (UTC+2), when a deep thermocline was expected at the location, and the second sampling was at approximately 18:00 h (UTC+2), when a shallow thermocline was anticipated. Preliminary results for 2021 showed that twice-daily sampling was not sufficient to properly capture daily variations and that it was necessary to sample at least four times per day during an intense ITW event. Therefore, in 2022, an adaptive sampling strategy was applied using forecasts from operational meteorological and oceanographic models (provided five days in advance) to predict an optimal well-developed ITW episode and to conduct four measurements per day during that period at approximately 06:00, 12:00, 18:00, and 24:00 h (UTC+2). The Regional Ocean Modeling System (ROMS), a 3D hydrostatic, nonlinear, free-surface, sigma coordinate, and time-splitting finite difference primitive equation model [28,29], was used to obtain 3-hourly outputs of temperature, salinity, and currents around Lastovo. More details on the operational Adriatic ROMS setup can be found in Janeković et al. [30]. Hourly wind fields were forecasted using the Weather Research and Forecast (WRF) model (https://www.mmm.ucar.edu/models/wrf) developed by the National Centre for Atmospheric Research and designed for operational forecasting and atmospheric research. Finally, wind data measured at Lastovo meteorological station (DHMZ; Fig. 1; latitude: 42° 46.10′ N, longitude: 16° 54.02’ E) were used to detect episodes of strong diurnal wind forcing in the area and relate them to temperature time series observed at Struga station.

The depths for the discrete sample collection were selected based on the *in situ* thermohaline profile. Samples for nutrient, Chl *a*, phytoplankton, and bacterioplankton analyses (light microscopy and flow cytometry) were collected from the same Niskin bottle and fixed as described by Matek et al. [19].

Zooplankton were sampled in two layers with opening–closing Nansen nets with mesh sizes of 53 μm and 200 μm: deep layer, from the seafloor to the thermocline, and surface layer, from above the thermocline to the sea surface (Table S1). Two HYDRO-BIOS WP2 closing nets (product ID 438,515) with a HYDRO-BIOS messenger-operated closing mechanism (product ID 438,520) were used. A subsample (ca. 50–100 ml) was taken for the extraction of environmental DNA (eDNA) and small ribosomal units of bacteria and

eukaryotes (16S rRNA and 18S rRNA genes), while the remaining sample was preserved in a 4 % formaldehyde seawater solution for light microscopy analyses. A small volume of the concentrated subsample collected with the Nansen net offered sufficient eDNA material and allowed quick subsequent laboratory processing in comparison to the sampling and filtration of large-volume water samples (e.g. 8–10 L of seawater), as performed by Matek et al. [19], while offering a resolution for bacterioplankton and zooplankton community analysis of equal quality. The eDNA subsamples were filtered on 0.2 μm pore-size polycarbonate filters (Cytiva Whatman Cyclopore, US) and immediately frozen in liquid nitrogen and transferred to the laboratory where they were stored at −80 °C until eDNA extraction.

2.2. Plankton community and nutrient analysis

Microphytoplankton (>20 μm) and nanophytoplankton (2–20 μm) were analyzed using light microscopy and photosynthetic picoeukaryotes (PPEs) and bacteria (photosynthetic cyanobacteria and heterotrophic bacteria) using flow cytometry, as described in Matek et al. [19].

Microzooplankton were divided using a Folsom plankton splitter (1/81/16 of the total catch) and analyzed using an inverted microscope (Olympus IMT-2) at 100× and 400× magnification. Mesozooplankton were counted from a representative sample of 1/32 of the total catch using a SMZ800 stereomicroscope and the sample was checked for rare species. Taxonomic identification was performed at the lowest possible level. The samples were processed in the laboratory according to standard zooplankton methods [31]. Abundance was expressed as individuals per cubic meter (ind. m^{-3}).

Nutrient, phosphate (PO_4), nitrate (NO_3), nitrite (NO_2), and silicic acid (SiO_4) concentrations were analyzed using an autoanalyzer (SEAL QuAAtro segmented flow AutoAnalyzer) and chlorophyll *a* using fluorometric analyses, as described by Matek et al. [19]. Enhanced concentrations of nutrients were observed (phosphate and nitrate were up to 2.19 and 10.25 μmol L^{-1}, respectively). To test those extremes, a z-score analysis was performed and all data with z score > ±3 were omitted (Fig. S1).

For data visualization and statistical analyses, the sampling depths were grouped according to the temperature data obtained from the CTD observations. Samples were grouped as follows: surface (T = 21.9–26.8 °C), thermocline (T = 17.0–21.9 °C), and deep layer (T = 15.2–17.0 °C) (Table S1).

2.3. NPP

Dissolved oxygen concentrations in the three along-isopycnal water layers (surface, thermocline, and deep layers) were averaged according to the analysis described in Section 2.2. Gross primary production (GPP) and corresponding respiration losses were estimated using a diel cycle for growth and mortality [32]. Temporally resolved NPP was estimated from the oxygen-derived difference between gross primary production and net loss according to Nicholson et al. [33].

2.4. eDNA isolation, amplicon sequencing, and bioinformatics

eDNA was extracted from polycarbonate filters using the DNeasy PowerSoil kit (Qiagen, Hilden, Germany) following the manufacturer's instructions with minor changes (Supplementary Material). Samples of total extracted DNA were sent to Novogene Co., Ltd. (Cambridge, UK) for 16S rRNA and 18S rRNA gene library preparation and amplicon next-generation sequencing; details are available in the Supplementary Material. Choosing universal small ribosomal subunit gene markers (16S and 18S rRNA genes, variable V4 regions) ensures quick and correct taxonomic identification for this interdisciplinary study, where resources were divided between physical, biochemical, and biological methodologies knitted together to describe ITW phenomena and their effect on biota.

The quality of the raw reads was verified using FastQC version 0.11.5 [34]. and visualized using the MultiQC tool (reports available at PUH data storage and management service, https://puh.srce.hr/s/ZSS2qz8ji5PStDj) for all samples together [35], after which the reads were processed using QIIME2 version 2021.11 [36]. The pipeline was composed of several steps: importing and demultiplexing of raw sequence data (fastq.gz), quality filtering and denoising using DADA2 plugin [37], and taxonomy assignment of the resulting amplicon sequence variances (ASVs) using Naïve Bayes classifier pre-trained on the latest version SILVA138 database [38] for prokaryotes and PR2 database for eukaryotes with 99 % Operational Taxonomic Unit (OTU) identity threshold [39]. The code is available at the PUH data storage and management service (https://puh.srce.hr/s/ZSS2qz8ji5PStDj). Because one of our objectives was to identify the possible impacts of ITW events on plankton communities, statistical analyses based solely on compositional (Bray-Curtis) or presence/absence (Jaccard) indices were not applied. Instead, a robust Aitchison distance matrix indicating log-fold changes and focusing more on rare taxa as key players [40] was calculated on 19 samples for each sequenced gene, with confidence level of 95 %. The two-way crossed Analysis of Similarity (ANOSIM) and Permutational Analysis of Variance (PERMANOVA) were used to test statistical significance (level of statistical significance, $p < 0.05$) between sample groups ('ITW'/'no ITW'; deep/surface layers and mesh sizes). Additionally, to achieve the third objective of the study of elucidating the functional ecological roles of bacterioplankton before, during, and after an ITW event, we applied FAPROTAX as a manually curated database that maps prokaryotic taxa according to their ecological roles in nature comes in handy when dealing with amplicon sequence data. These state-of-the-art tools were applied to enable a comprehensive approach of metabarcoding a single gene as a powerful tool in this interdisciplinary study. Details on the filtering and preparation of datasets for diversity analyses with *q2-diversity*, *deicode* [40,41] plugins, and ecological function annotation using the FAPROTAX database [42] are available in the Supplementary Material. Raw sequences were deposited in the European Nucleotide Archive (ENA) under project number PRJEB63220.

2.5. Statistical analyses of physical-chemical data and zooplankton community

Statistical analyses were performed on 180 samples and results with a confidence level of 95 % were considered statistically significant. Prior to analysis, biotic data were log-transformed to run similarity and correlation tests between different plankton groups and environmental variables, whereas physicochemical parameters were normalized and standardized to convert all variables to a common dimensionless scale. ANOSIM test is a non-parametric method that uses only ranks; therefore, it is suitable for testing similarities between different abiotic and biotic data. ANOSIM (level of statistical significance, $p < 0.05$) was applied to Euclidian distance resemblance matrices of log-transformed and normalized nutrient concentrations (μmol L^{-1}) and to log-transformed micro- and nanophytoplankton (cell L^{-1}) and picophytoplankton (cell mL^{-1}) abundances to test similarities among sampling groups before and after ITWs in the stratified water layer (Primer 7.0; Primer-E Ltd. 2021, Auckland, New Zealand). Canonical correspondence analysis (CCA) was performed in the R programming language using the ggvegan package. CCA is a type of multivariate analysis that considers multiple variables simultaneously and is an ordination technique that represents the relationships between species abundance and environmental variables in a low-dimensional space. Furthermore, it provides correlations between biotic and environmental data while assessing the significance of environmental variables in explaining the variation in species composition. CCA was run on the log-transformed phytoplankton and picophytoplankton cell counts (cell L^{-1} and cell mL^{-1}, respectively), while the environmental dataset (nutrients concentrations (μmol L^{-1}), Chl *a* (μg L^{-1}), and temperature (°C)) were log transformed, normalized, and standardized. Variance inflation factors (VIF) were calculated for each parameter in the environmental data to exclude highly correlated parameters (VIF >10) from the model. There are no redundant constraints. Analysis of variance (ANOVA) was used to test the statistical significance of the CCA model ''biotic dataset ~ environmental dataset'' (level of statistical significance, $p < 0.05$) and of the constrained axes (CCA1 and CCA2). The CCA scores (environmental biplot scores and species-weighted average scores) were visualized using the

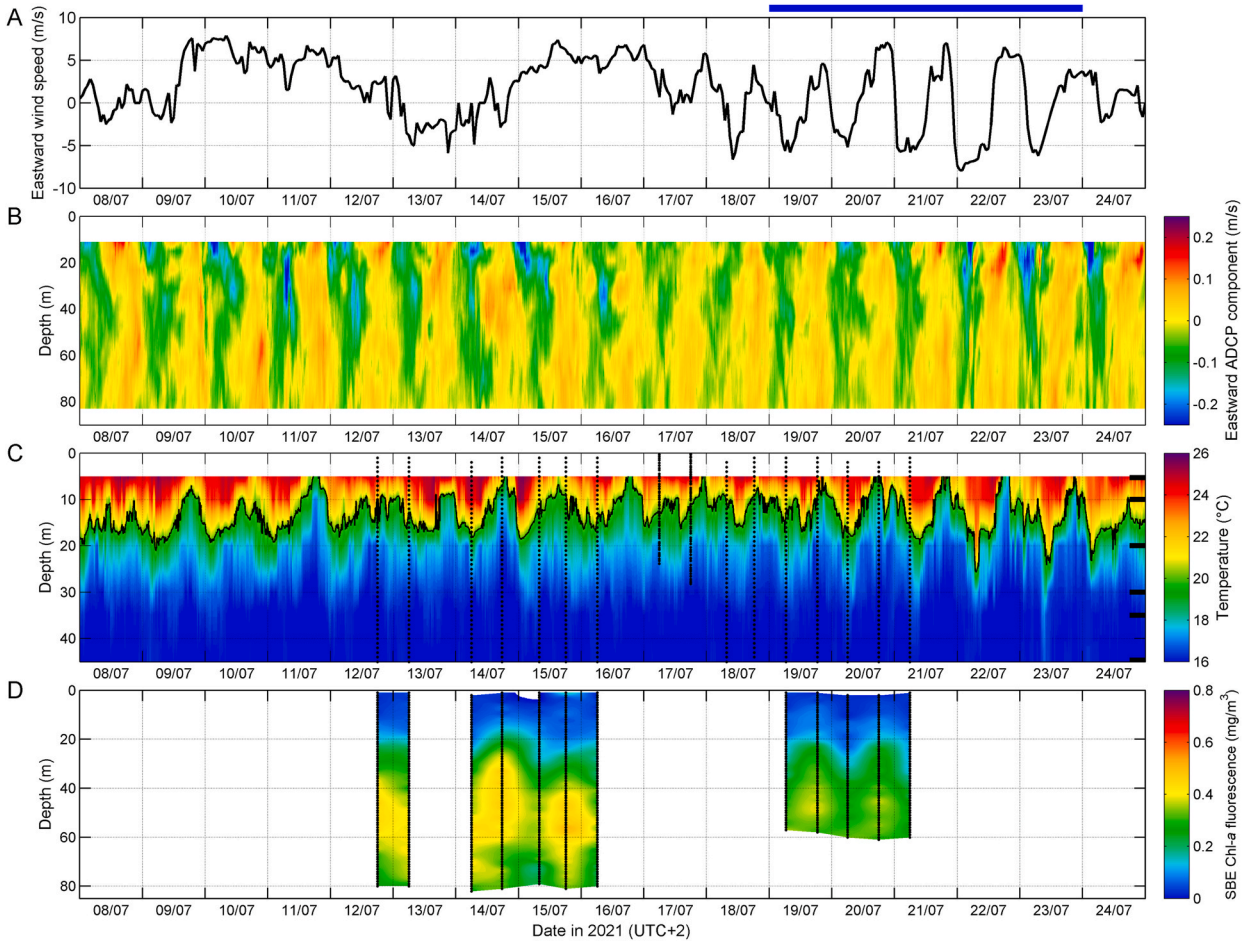

Fig. 2. Observations in July 2021. Eastward wind speed (A), eastward ADCP component (B), temperature data recorded on loggers from the cliff at S1 station (C), and Chl *a* fluorescence (Chl F) vertical profiles recovered from CTD casts (D) in July 2021. The period of the ITW event is indicated by a blue horizontal line above panel (A). Vertical dotted lines in (C) and (D) indicate CTD casts. Black horizontal ticks in the right part of panel (C) indicate deployment depths of temperature loggers, while the thick black contour indicates the 20 °C isotherm. (For interpretation of the references to colour in this figure legend, the reader is referred to the Web version of this article.)

package ggplot2.

The dominant taxa of mesozooplankton identified using the morphological approach were statistically analyzed using SIMPER according to the different sampling layers. Compositional bar plots were constructed using Grapher 7.0 (GrapherTM from Golden Software, LLC).

3. Results

3.1. Thermocline oscillations and detection of ITWs

This section presents wind data from the Lastovo meteorological station and oceanographic measurements collected at the Struga (S1) and ADCP stations during the 2021 and 2022 campaigns. The eastward wind component was selected as a good proxy for detecting significant sea-land-breeze forcing in the Lastovo area, during which winds mostly blow from the NW in the afternoon and from the NE at night.

A field experiment was conducted in 2021 between 12 July (late afternoon) and 21 July (early morning). Sampling was conducted twice a day, with some measurements missing due to logistical problems. However, the strongest diurnal wind episode occurred between 19 and July 23, 2021, peaking on 21 July (Fig. 2A). The currents assessed by the eastward component, that is, along the southern Lastovo coast (Fig. 2B) and temperature logger data from Struga cliff (Fig. 2C), indicated that this wind episode resulted in enhanced diurnal currents in the upper part of the water column and diurnal thermocline oscillations of 20 m on 22 and July 23, 2021. Diurnal oscillations were also detected in Chl F data (Fig. 2D). Because the field measurements were completed by that time, ship-based oceanographic sampling did not cover the most significant part of the ITW event in July 2021.

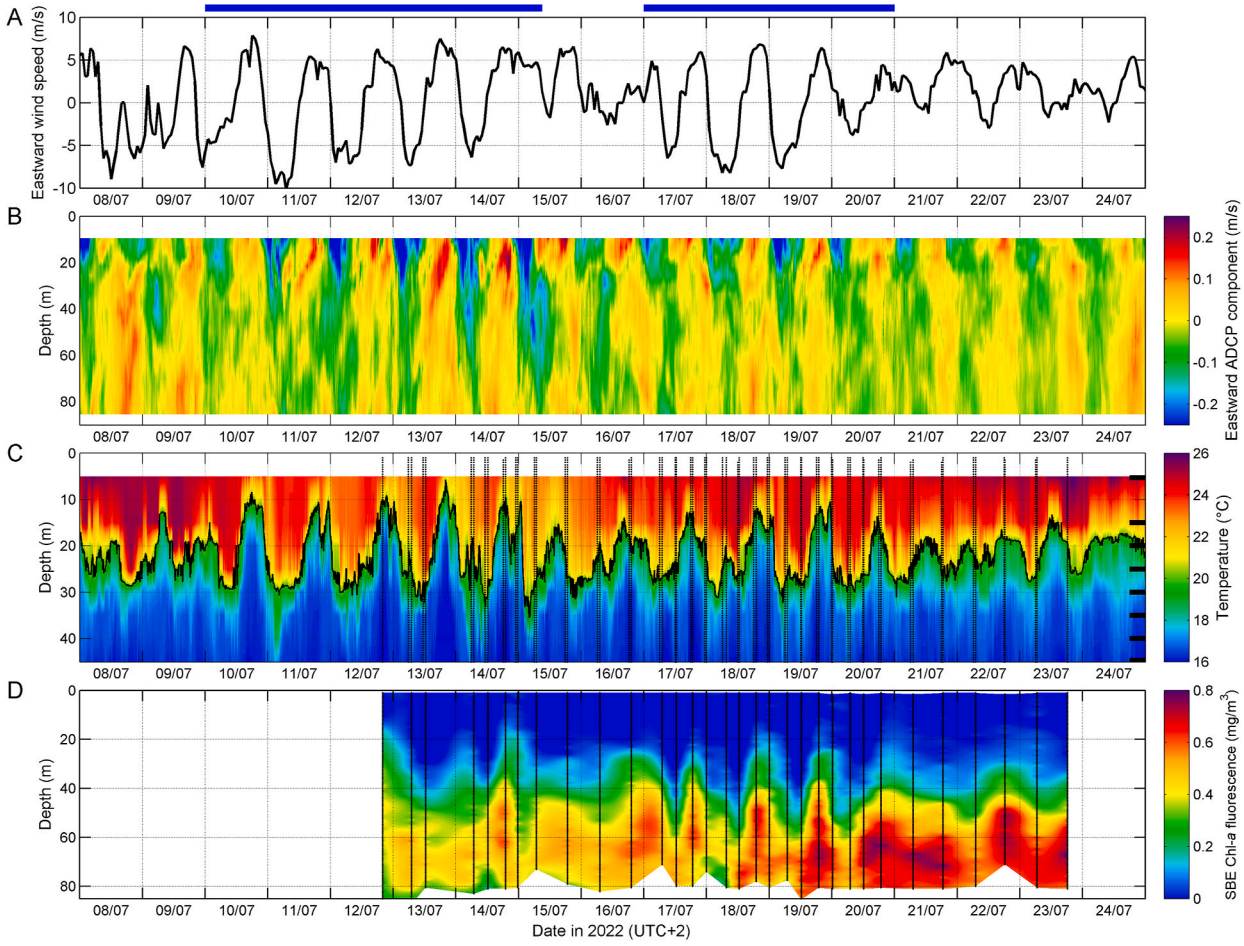

Fig. 3. Observations in July 2022. Eastward wind speed (A), eastward ADCP component (B), temperature data recorded on loggers from the cliff at S1 station (C), and Chl *a* fluorescence (Chl F) vertical profiles recovered from CTD casts (D) in July 2022. The periods of two ITW events are indicated by blue horizontal lines above panel (A). Vertical dotted lines in (C) and (D) indicate CTD casts. Black horizontal ticks in the right part of panel (C) indicate deployment depths of temperature loggers, while the thick black contour indicates the 20 °C isotherm. (For interpretation of the references to colour in this figure legend, the reader is referred to the Web version of this article.)

The 2022 field campaign included operational meteorological and oceanographic models. Their results were analyzed daily and used to predict ITW events in advance and plan more intense sampling (four times per day) during the events. The measurements from 2022, corresponding to the same period as in 2021, are presented in Fig. 3. The field experiment began on July 12, 2022 (late afternoon), during an intense ITW event that lasted from 10 to July 15, 2022. ITW episodes in the measurements and models were defined by the amplitudes of the related diurnal wind and thermocline oscillations. An ITW event was considered significant when the diurnal amplitudes of the eastward wind component were larger than 6 m s^{-1}, with the range of concurrent thermocline oscillations exceeding 12 m. However, the winds during this episode were so strong that they mostly prevented fieldwork and four-times-per-day sampling was achieved only on July 14, 2022. The first prediction of the next ITW episode was made at that time. Consequently, the decision was made to start intense sampling on July 17, 2022, as long as the models showed strong diurnal wind and temperature oscillations. This second ITW event lasted from 17 to July 21, 2022, with somewhat weaker diurnal winds than those during the first event (Fig. 3A), but still resulted in strong diurnal currents close to the surface (Fig. 3B) and the excitation of diurnal temperature oscillations, peaking on 18 and July 19, 2022 (Fig. 3C). More frequent ship-based measurements resulted in clear observations of pronounced vertical movements in the deep chlorophyll maximum (DCM; Fig. 3D). The experiment was continued until July 23, 2022 (early morning).

Because the ITW event observed in 2021 developed at the end of the field experiment (Fig. 2), further analyses and comparisons with the biogeochemical parameters in this study were performed only for 2022, when the experiment captured the end of an intense ITW event in the first half of July and then covered the period before, during, and after another significant ITW episode in the second part of July (Fig. 3).

3.2. Nutrient concentration and plankton community response to the ITW event

In the stratified water column, differences were observed between the three layers based on thermohaline properties and nutrient concentrations (Figs. S2 and S3). The depths of the layers varied over the study period following pronounced thermocline oscillations (Table S1). Average nutrient concentrations were low (Table 1), with the highest values observed in the deep layers (Fig. 4). Higher values were detected throughout the water column on 13 July and from 18 to 20 July, reaching maximum concentrations of phosphate (0.25 μmol L^{-1}), nitrite (0.14 μmol L^{-1}), and nitrate (1.92 μmol L^{-1}) (Table 1, Fig. 4). Silica did not show the same trend of increasing concentration in the surface and thermocline layers. Box-whisker plots showed smaller changes in nutrient concentrations in the deep layers, whereas the surface and thermocline layers showed high variability (Fig. S4). Statistical analyses were performed to test the observed temporal and spatial variations (two-way crossed ANOSIM test). Although outlier values were observed during the ITW events (Fig. 4), the ANOSIM test did not show changes in the nutrient concentrations before and after the ITW events; however, the results were not significant (Table S2). However, vertical dissimilarity in nutrient concentrations was confirmed, with significant differences between the surface and thermocline layers and the deep layer (Table S2).

Chlorophyll *a* was low in the surface and thermocline layers, with maximum values below the thermocline, forming a pronounced DCM. The depth of the DCM was variable and the most pronounced thermocline oscillations coincided with the DCM oscillations at depths between 20 and 80 m (Fig. 3D).

Distributions of micro- and nanophytoplankton abundances did not show distinctive spatial or temporal patterns, reaching maximum abundances of 7.7×10^3 cells L^{-1} and 1.8×10^4 cells L^{-1}, respectively (Fig. 5). Slight increases in the abundance of microphytoplanktons were recorded in the deep layer, whereas nanophytoplanktons dominated the community throughout the water column. These observations were supported by a two-way crossed ANOSIM test and only statistically significant results are discussed (level of statistical significance, $p < 0.05$) (Table S2). The test confirmed a dissimilarity in picoplankton abundance in the stratified water column and no distinct vertical distribution of nano- and microphytoplankton (Table S2). There were no differences in the pico-, micro-, or nanophytoplankton abundances before and after the ITW events (Table S2).

The CCA confirmed distinct water layers, where the deep layer was mostly described by enhanced nitrite, nitrate, and silicate concentrations, the thermocline layer by enhanced phosphate, and the surface layer by the highest temperatures (Fig. S5). The biplot scores of the environmental variables, species-weighted average scores, and constrained axis eigenvalues are presented in the Supplementary Material (Table S3). The constrained axis explained 88.9 % ($p = 0.002$) of the picoplankton community variability and only 11.7 % ($p = 0.001$) of the micro- and nanophytoplankton variability (Fig. S5A), indicating a faster response of picoplankton to

Table 1
Average (Avg), standard deviation (SD), maximum (Max), minimum (Min), and number of samples (N) for physicochemical parameters during the 2022 field experiment at Lastovo Island, Struga station (S1): temperature, salinity, phosphate (PO_4), nitrate (NO_3), nitrite (NO_2), silicate (SiO_4) and chlorophyll *a* (Chl *a*).

Parameter	Avg	SD	Min	Max	N
Temperature (°C)	19.51	3.60	15.19	26.79	180
Salinity	38.97	0.05	38.87	39.10	180
PO_4 [μmol L^{-1}]	0.02	0.02	0.007	0.25	179
NO_2 [μmol L^{-1}]	0.04	0.03	0.003	0.14	180
SiO_4 [μmol L^{-1}]	0.66	0.38	0.32	1.92	178
NO_3 [μmol L^{-1}]	0.42	0.41	0.05	1.92	178
Chl *a* [μg L^{-1}]	0.39	0.38	0.01	1.96	177
Redfield ratio	24.52	23.03	0.01	101.6	180

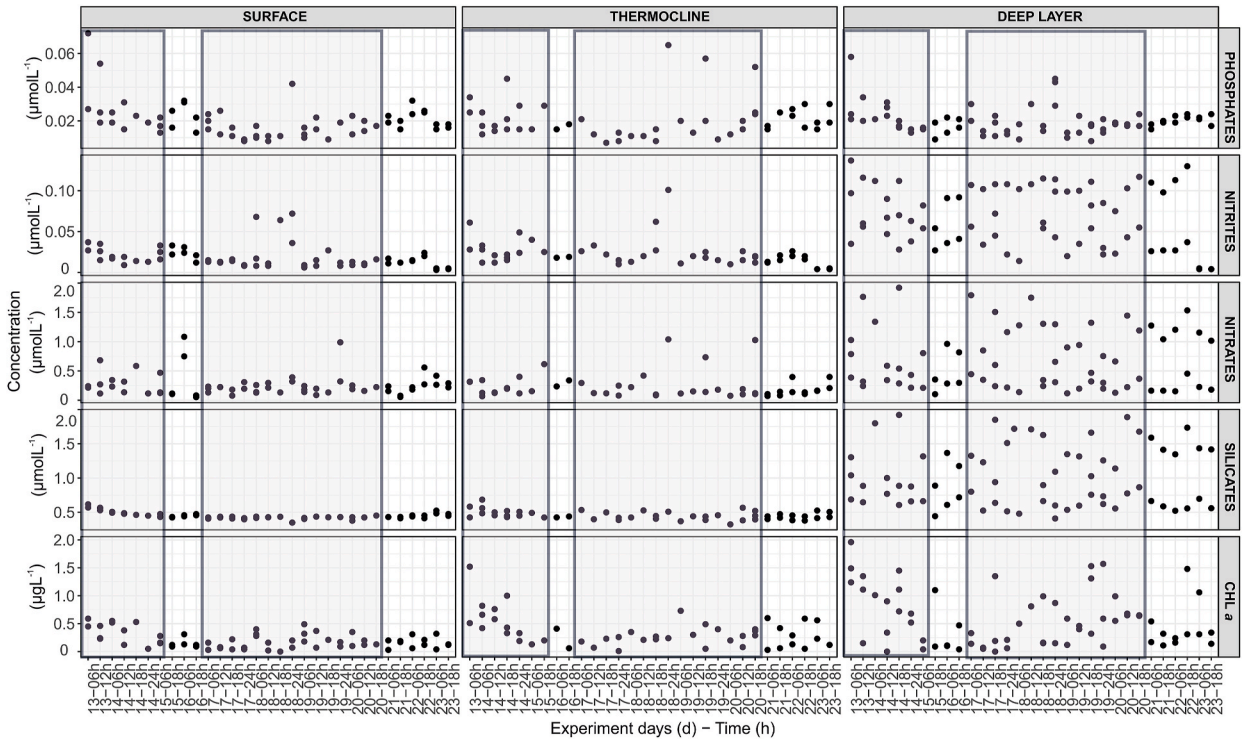

Fig. 4. Temporal variations in nutrient (phosphate (PO_4), nitrate (NO_3), nitrite (NO_2), silicate (SiO_4)) and chlorophyll *a* concentrations at Station S1 in the period between 13 and July 23, 2022. The peak value of phosphate concentration (0.25 μmol L^{-1}) detected in the thermocline layer was omitted from the graph to increase the visibility of fine temporal phosphate concentration changes in the surface and thermocline layers. Periods of the ITW events are highlighted.

changes in the environment. The ANOVA test (level of statistical significance, $p < 0.05$) confirmed significantly distinct vertical distributions of picoplankton ($p = 0.001$). *Synechococcus*, heterotrophic bacteria, and PPEs were abundant in the surface and thermocline layers, whereas the deep layer was dominated by *Prochlorococcus* (Fig. 5 and Fig. S5B). There was no clear separation of larger plankton fractions in the water column; however, the ANOVA test confirmed significant correlations ($p = 0.01$) of microphytoplankton with higher concentrations of nitrate, silicate, and Chl *a* and nanophytoplankton with higher temperature and phosphate concentrations (Fig. S5A).

Microzooplankton showed high overall diversity, with large numbers of tintinnids and juvenile individuals (nauplii, copepodites, and larvae). Because of the interest in larger copepods and mesozooplankton in general and their association with bacterial communities assessed using eDNA approaches, further analyses were performed on a microscopic dataset of the meso-fraction. A total of 80 mesozooplankton taxa in the net tows were determined: 72 in the upper layer and 73 in the lower water layer, with 10 characterized as dominant (abundances representing more than 50 % of the community) (Table S4). There was a clear separation between the deep and surface layers, which was corroborated by the dissimilarity index calculated using SIMPER (Table S4). Calanoid copepods *Centropages typicus* (Krøyer, 1849) and *Paracalanus parvus parvus* (Claus, 1863) mostly graze on small organisms (diatoms, dinoflagellates, coccolithophorids and small animal larvae), along with nano-size filter feeding appendicularian *Oikopleura (Coecaria) longicauda* (Vogt, 1854) were dominant in the deep layers, while the rest of the herbivorous filter feeding cladocerans and omnivore cyclopoid copepods, such as *Oithona* spp. (Baird, 1843), prevailed in the surface layers (Table S4, Fig. S6). *Evadne* spp. (Lovén, 1836) and *Corycaeus* spp. (Dana, 1845) were only identified morphologically, whereas the remaining dominant taxa were also identified among the ASVs. Strong shifts in daily dominance in mesozooplankton communities were observed, with the most obvious changes from herbivorous filter-feeding cladocerans during the ITW events to animal-prey calanoid copepods and omnivorous *Oithona* juvenile and adult individuals after the ITW events (Fig. S6).

3.3. Response of NPP to ITW event

Oxygen variability was quantified using the four daily CTD profiles, with data averaged for the surface, thermocline, and deep layers (see Section 2.3). The model, with sinusoidal fits spanning 72 h each and centered at 6 h intervals, had significant correlations only for the thermocline layer (averaged between the 27.29 and 28.54 kg m^{-3} isopycnals) (Fig. 6A), with $p < 0.05$ and r^2 values ranging from 0.20 to 0.81. The data also showed departures from the model, likely owing to lateral advection and other sources of variability. Gross primary oxygen production and losses were derived from the model (Fig. 6B) and were significantly correlated ($r^2 =$

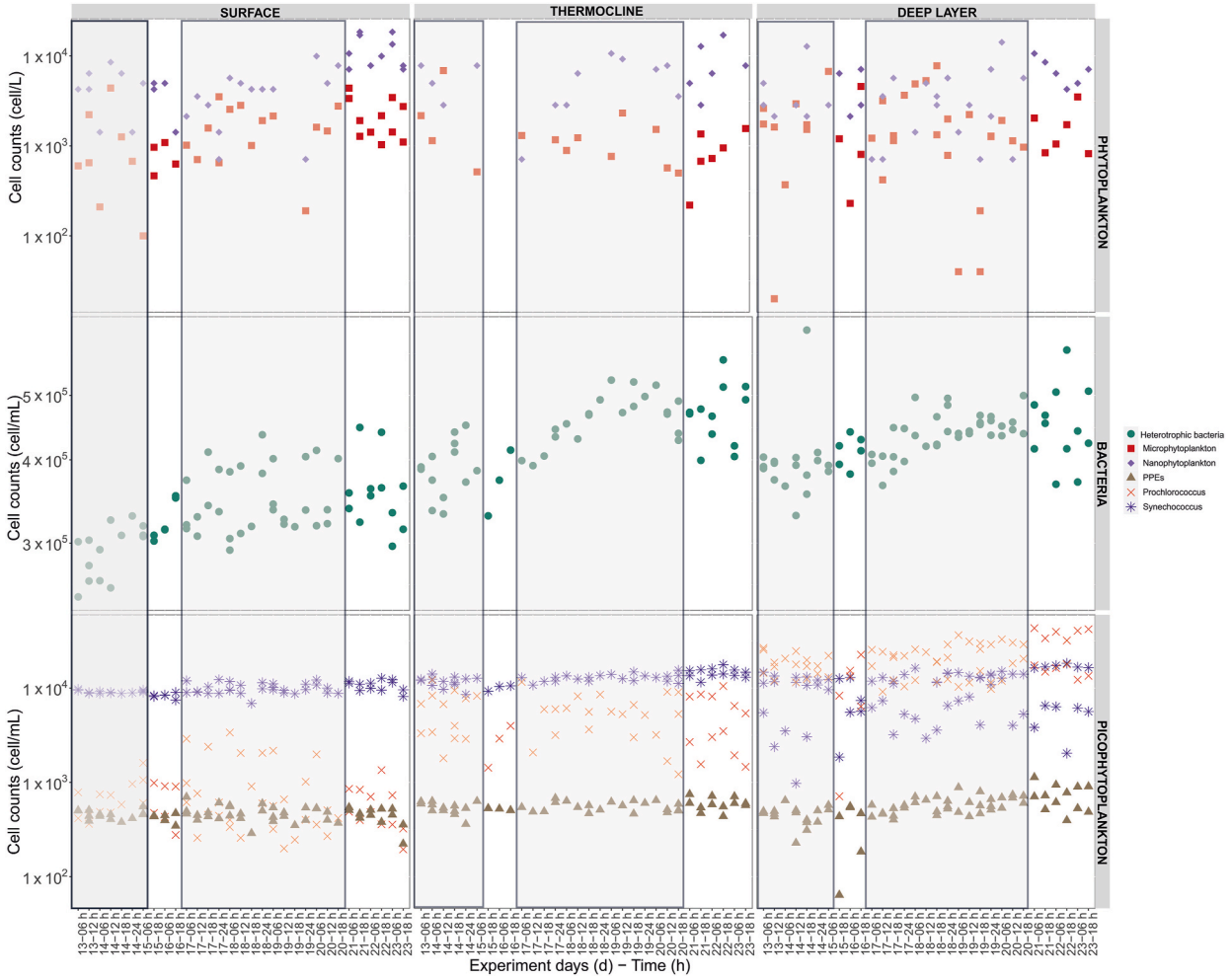

Fig. 5. Temporal distribution of plankton abundances at Station S1 in the period between 13 and July 23, 2022. Periods of the ITW events are highlighted.

0.94) with a slope (GPP versus losses) of 1.59. The strong correlation between the two reflects the coupling between respiration processes and primary production. The difference between the two provides a measure of NPP. The model suggests that NPP increased on July 17, 2022, and reached a maximum value on July 20, 2022, which corresponds to the period of the ITW event (Fig. 6C).

3.4. eDNA overview statistics

Amplicon sequencing of 19 net-towed samples resulted in a total of 2,577,627 raw reads, of which 1,314,573 were cleaned (quality filtered, denoised, merged, and depleted of chimeras) for the 16S rRNA gene, and 2,578,382 raw reads from which 1,510,943 were cleaned and used in the analyses of the 18S rRNA gene (Table S5). After DADA2 denoising and the removal of rare ASVs (singletons, doubletons, short reads, and chimeras), a final number of 1821 (16S) and 3353 (18S) representative ASVs were obtained and used for downstream analysis. Rarefaction analysis revealed that the denoised, quality-filtered, and chimera-free sequences were sufficient to reach saturation in each sample.

3.5. Primary and secondary producers, grazers, and decomposers in the plankton community (eDNA analysis)

Higher diversity richness in samples was observed in the eukaryotic dataset (Shannon index: 2.63–6.99) in comparison to the bacterial dataset (1.15–4.03), although general distributions were relatively similar (Figs. S7 and S8). Pielou's evenness index indicated a higher homogeneity of bacterial samples (0.14–0.61, Fig. S7) than in the eukaryotic dataset (0.35–0.88, Fig. S7), while Faith's phylogenetic diversity in both datasets showed a wide range with indications of evolutionary diverse taxa (16S rRNA 4.59–31.39, Fig. S7; 18S rRNA 12.98–22.92, Fig. S8), with maximum values in the bacterial dataset. Observed ASVs are in relation to the richness index values higher in the eukaryotic dataset in comparison to the bacterial dataset (Table S3). Kruskal-Wallis statistical test (level of

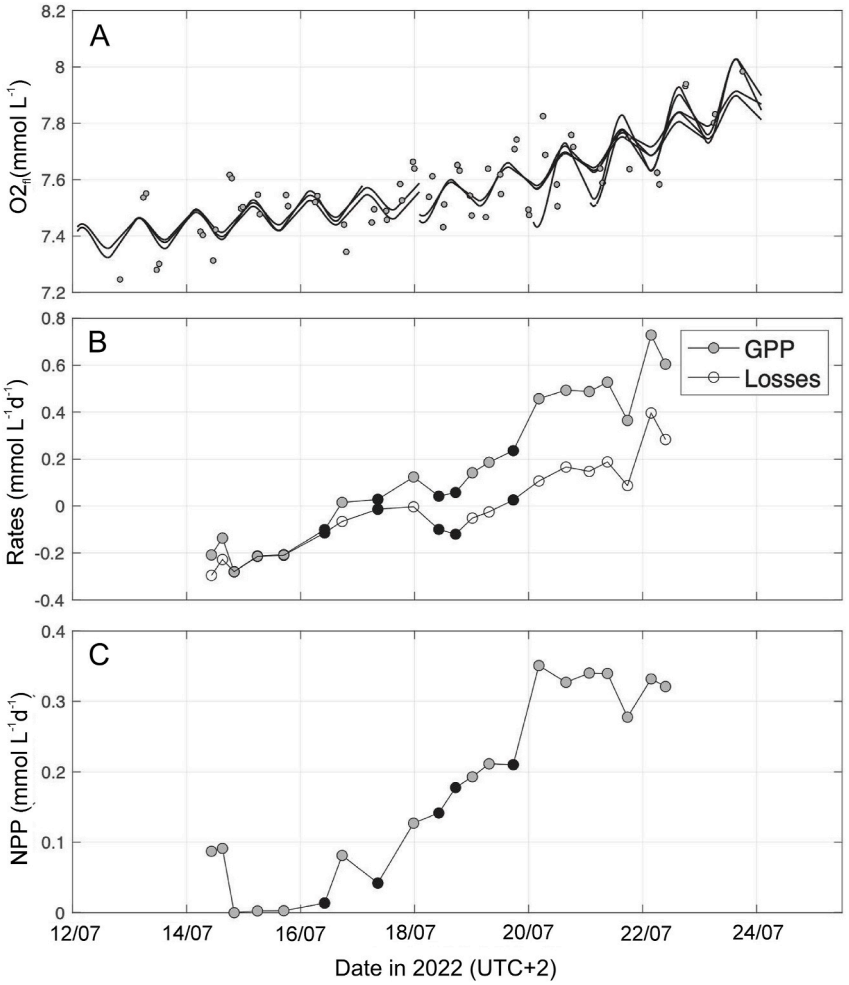

Fig. 6. Diel variability in oxygen concentrations in the thermocline layer from CTD casts (circles, averaged between the 27.29 and 28.54 kg m^{-3} isopycnals) during the intensive sampling period between 14 and July 22, 2023 (panel A). Solid lines are sinusoidal fits spanning 72 h each, centered at 6 h intervals. Gross primary oxygen production (gray circles) and losses (open circles) were estimated from the fitting model, with black points indicating non-significant fits where $p < 0.05$ (panel B). Oxygen-based NPP estimated from the difference between GPP and losses is shown in panel C.

statistical significance, $p < 0.05$) results were not significant for the 'ITW'–'no ITW' sample group in each tested alpha diversity index in the bacterial or eukaryotic datasets (Figs. S7 and S8, bottom panel *p*-value).

A robust Aitchison's distance principal component analysis (rPCA) of the bacterial dataset revealed a strong divergence between sample groups corresponding to samples collected during and after ITW events (first axis explaining 51.83 %; Fig. 7A; ANOSIM and PERMANOVA test results shown in Table 2, level of statistical significance, $p < 0.05$). However, there was no significant difference between the net tows in the deep and surface layers or between the mesh sizes (Fig. 7A, Table 2). In the 18S rRNA gene dataset, rPCA showed scattered samples without significant dissimilarity between sample groups (first axis explaining 58.66 %, Fig. 7B, statistical test results in Table 2); without a significant dissimilarity between sample groups. Although the sample groups divided by mesh sizes were not significantly different ($p = 0.08$), there was indication of a putatively significant separation of microbial eukaryotes (Table 2).

Compositional rPCA biplots showing eight features with the highest PC1 loading scores revealed that the presence of ITW events explained two clusters in the bacterial dataset (Fig. 7A) better than in the eukaryotic dataset (Fig. 7B). The list of the strongest contributing bacterial features (5 % of all features) to sample clustering, along with the log ratios of feature loadings, as visualized by QURRO, is shown in Tables S6A–B. Additionally, the list of the strongest contributing eukaryotic features (10 % of all features) to sample clustering along with the log-ratios of feature loadings, as visualized by QURRO, is shown in Tables S7A–B. Features are classified into 'Numerator' and 'Denominator' clusters, showing which taxa contribute the most to the diversification of two sample groups. Therefore, the clustering of the 'ITW' sample group in the bacterial dataset was highly influenced by *Pseudomonas*, *Pseudoalteromonas*, *Vibrio,* and uncultured Campylobacterales as shown in Fig. 7A. Other taxa also showed high log ratios in favor of the 'ITW' sample group: *Poseidonibacter*, *Marinobacterium*, *Rubivirga profundi*, *Marinomonas*, *Devosia*, *Cobetia*, *Kocuria,* and *Sinobacterium* (Table S7A). On the other hand, genera *Sulfitobacter*, *Limimaricola*, *Paracoccus*, *Dokdonia*, *Roseburia, Caenispirillum*, *Alteromonas,* and

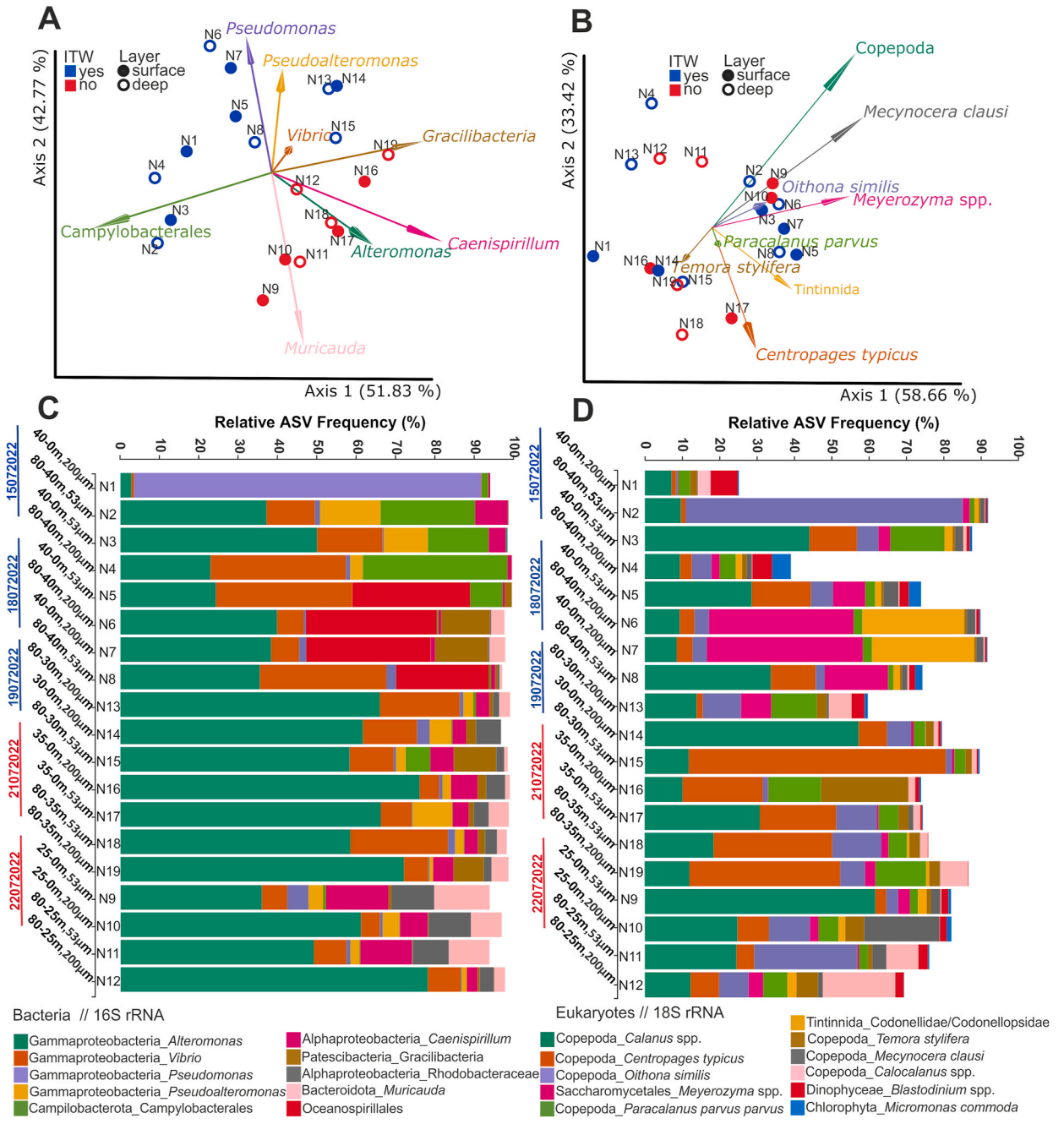

Fig. 7. Robust Aitchison principal component analysis (rPCA) plot of bacterial (A) and eukaryotic (B) communities based on 16S rRNA and 18S rRNA genes taxonomy classification and feature (ASV) abundances. Blue samples correspond to the 'ITW' group and red samples correspond to the 'no ITW' group while circles correspond to surface layers and rings to deep layers. Euclidian distance from the origin is represented by arrows. Taxonomic bar plots with the relative abundance of ASVs (%) of bacterial (C) and eukaryotic (D) communities with the highest contributing taxonomic groups (bacterial 10, eukaryotic 12) for each sample indicated on the vertical axis. The remaining taxa contributing up to 100 % are not shown. (For interpretation of the references to colour in this figure legend, the reader is referred to the Web version of this article.)

Muricauda, family Saccharospirillaceae, and phyla Gracilibacteria, visible in Fig. 7B, had the highest loading scores to the 'no ITW' sample group (Table S6A). Eukaryotic samples did not show strong clustering along the PC1 axis based on the presence of ITW phenomena (Fig. 7B). Many taxa yield loading scores in the 'Numerator' and 'Denominator' clusters, therefore preventing strong diversification, which is confirmed with insignificant results from the two-sided *t*-test (level of statistical significance, $p < 0.05$) (Tables S7A–B).

Gammaproteobacteria was the most frequent group in all samples, having relative abundances from 51.8 to 88.6 % in the 'no ITW'

Table 2
Pairwise statistical test values on robust Aitchison distance of sample groups from 16S rRNA and 18S rRNA datasets; ***strongly significant; *putatively significant.

Sample group	PERMANOVA		ANOSIM	
	p-value	Pseudo-*F*	*p*-value	Rho
16S rRNA				
'ITW'–'no ITW'	0.001***	10.62	0.001***	0.53
Deep–Surface	0.93	0.08	0.97	−0.09
200–53 μm	0.13	2.28	0.27	0.03
18S rRNA				
'ITW'–'no ITW'	0.58	0.52	0.68	−0.05
Deep–Surface	0.45	0.86	0.45	−0.01
200–53 μm	0.08*	2.58	0.18*	0.05

group and from 61.8 to 94.1 % in the 'ITW' group (Fig. 7C). In sample N1, most Gammaproteobacteria are identified as genus *Pseudomonas* (88 %), while in other 'ITW' samples, Gammaproteobacteria were mostly equally divided into genera *Pseudoalteromonas* and *Vibrio* and family Oceanospirillales (genus *Cobetia*) (Fig. 7C). In the 'no ITW' sample group, *Pseudoalteromonas* and *Vibrio* are replaced with *Alteromonas* (59.5–73.1 %) (Fig. 7C). Another important contributor to the clustering of the 'ITW' sample groups was the family Campylobacterales with a maximum relative abundance in sample N4 (33.7 %, Fig. 7C). *Caenispirillum* (Rhodospirillaceae) contributed to the 'no ITW' sample group, with a maximum relative abundance in sample N9 (10.7 %), whereas in the 'ITW' sample group, it reaches a maximum of 6 % of total ASVs in N14 (Fig. 7C). Along with *Caenispirillum*, *Muricauda* (Flavobacteriaceae) also bloomed at the end of the experiment (July 22, 2022) and contributed to the separation of the 'no ITW' sample group with relative abundances from 1.2 % in N12 to 10 % in N9 (Fig. 7C). Gracilibacteria were more frequent in the 'ITW' sample group (~1–13.5 %), although a high relative abundance was observed in N19 (7.7 %) (Fig. 7C).

The eukaryotic community during ITW events was predominantly composed of Class Copepoda, (8–57.6 %) and Saccharomycetales (genus *Meyerozyma*), with relative abundances of 8.7–42 % in N5–N8 collected at the peak of the event (Fig. 7D), and Tinntinida (Codonellidae/Codonellopsidae), with maximum relative abundances in N6 and N7 (27.4 and 27.5 %, respectively; Fig. 7D). *Centropages typicus* mostly shaped the 'no ITW' sample group where it had high relative abundances (4.8–40.6 %, Fig. 7D), while genus *Oithona* was present in both sample groups with an absolute dominance in sample N2 (74.6 %) taken at the end of the first event (July

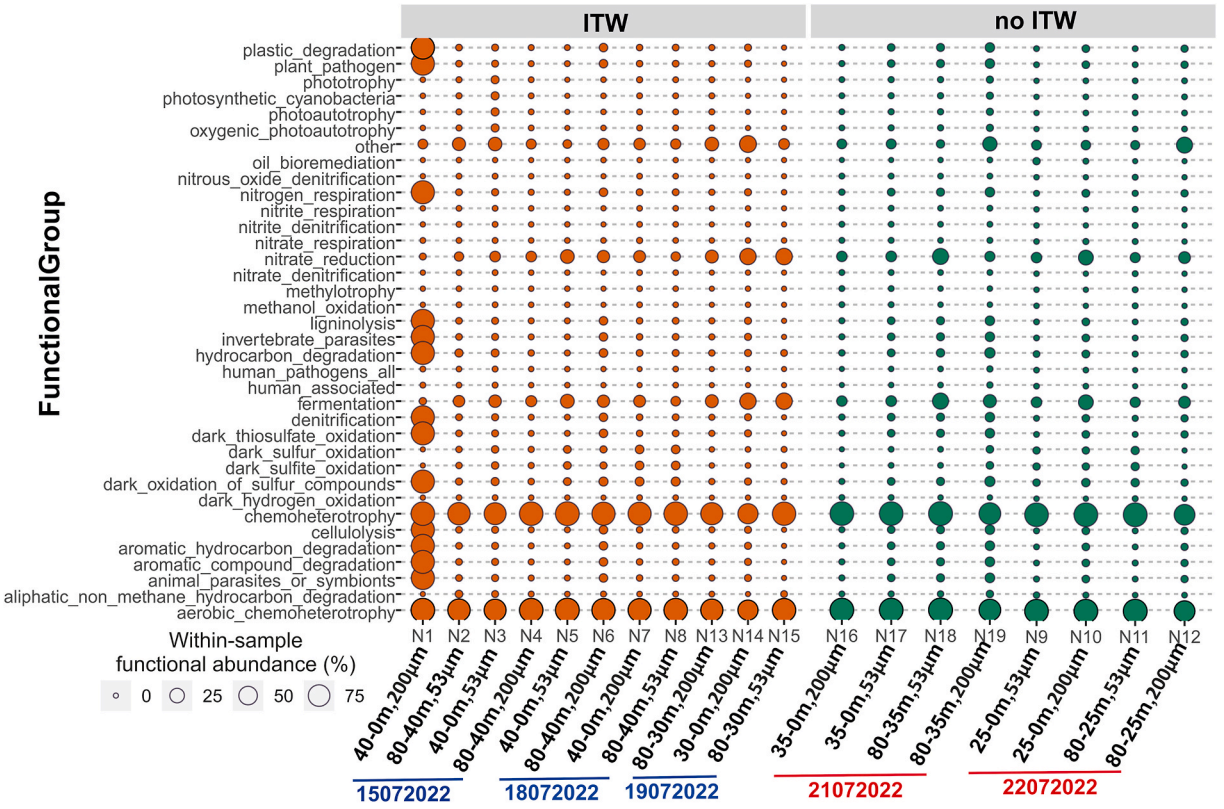

Fig. 8. Bubble plot representing bacterial functional groups from samples collected during and after the ITW episodes.

15, 2022) and beginning of stabilization period before the second event (Fig. 7D). Species from the genus *Oithona*, such as *O. similis* Claus, 1866, have log-ratios along axis 1 in rPCA in favor of the 'no ITW' sample group (Table S7A), while unidentified *Oithona* species are characterized as 'Denominator,' in favor of the 'ITW' sample group (Table S7A). *Temora stylifera* (Dana, 1849) was most abundant in N16 (23.5 %), slightly contributing to the 'ITW' samples (Fig. 7D–Table S7A). The dinoflagellates (*Blastodinium* spp. Chatton, 1906) and chlorophytes (*Micromonas commoda* Baren, Bachy & Worden, 2016) had higher relative abundances during ITW events (maximum of 8.7 % in N14 and maximum of 10.2 % in N4, respectively; Fig. 7D). *Mecynocera clausi* Thompson I.C., 1888 had a maximum of 20.3 % relative abundance in N10 and in the rest of the 'no ITW' period had <5 % of relative abundance, while during the ITW event, its relative abundances were between 1 and 4 % (Fig. 7D). Additionally, one more genus, *Calocalanus* Giesbrecht, 1888, had a higher relative abundance in the 'no ITW' samples (2–19.5 %) compared to ITW samples (1–6%) (Fig. 7D). The smallest contribution to sample clustering, *i.e.*, the most regularly present copepod, was *Paracalanus parvus parvus*, whose omnipresence was quantified by relative abundances ranging from 2 to 14.2 % in the 'no ITW' sample group and 1.3–14.6 % in the 'ITW' group (Fig. 7D).

3.6. Ecological functional profiling of bacterial communities during and after the ITW event

Functional profiles of bacterial communities in zooplankton net tows during and after ITW events are presented in Fig. 8. We detected 751 features (OTUs) clustered into 93 functional groups, of which 36 were represented by at least one record (0.001 %) (Fig. 8). Most functions represented degradation processes or processes associated with elevated NPP, including nitrogen respiration, nitrate reduction, fermentation, chemoheterotrophy, and aerobic chemoheterotrophy (Fig. 8). Functional groups were equally distributed between the 'ITW' and 'no ITW' sample groups, with slightly increased relative abundances during ITW events except in N1 (surface layer collected with 200 μm mesh size net at the end of the first ITW episode on July 15, 2022). This sample showed high bacterial activity associated with microplastic degradation, ligninolysis, nitrate respiration, parasitism, denitrification, plant pathogens, and cellulolysis (Fig. 8).

4. Discussion

4.1. Physicochemical and NPP variations during ITW event

Here, we present a multidisciplinary study that includes moored- and ship-based measurements to gain insights into the complex interactions in marine ecosystems and the potential impact of physical oceanographic phenomena on biological communities. Moored measurements offer fine-scale temporal resolution and were combined with fine-scale ship-based sampling with temporal resolution determined *in situ*, following real-time forecasts based on oceanographic and hydrographic models.

The 2021 survey at Lastovo Island was based on a twice-daily sampling regime (around 06:00 and 18:00 UTC+2), which was insufficient to adequately observe daily variations during an intense ITW event; the experiment ended while the ITW event was still developing. The 2022 experiment included daily operational meteo-oceanographic forecasts around Lastovo, enabling the prediction of an intense ITW episode and increasing the sampling effort to four measurements per day during the entire ITW event. The average thermocline depth at Struga differed between the July 2021 and July 2022 experiments. The average 20 °C isotherm depth in July 2021 was slightly deeper than 10 m, whereas it was approximately 20 m during the same period in July 2022. When the thermocline is deeper, the range of ITW isotherm oscillations is larger [43], which is evident from the July 2022 oceanographic data, when the thermocline oscillations were more pronounced than in July 2021.

This also emphasizes the importance of understanding changes in thermohaline properties in future climates when water column stratification is expected to increase. Such changes could alter the ITW resonance parameters around the island of Lastovo and potentially shift periods with intense ITW events or even reduce their occurrence during the stratified season. For example, the July 2022 experiment occurred between two marine heat waves. The end of the first heat wave is visible in Fig. 3C, on 8–9 July, and it was a continuation of a prolonged period with significantly higher-than-usual sea surface temperatures along the eastern Adriatic coast [44]. The experiment mostly took place under average sea surface temperature conditions, whereas the second heat wave started after 23 July (Fig. 3C). Coincidently, the abrupt change in meteorological and oceanographic conditions at the end of the first July 2022 decade shifted the local thermocline parameters closer to resonance. Additionally, when meteorological conditions stabilized, two intense sea and land breeze episodes occurred between 10 and July 20, 2022 (Fig. 3A). Therefore, presuming that the existence of ITWs around the island of Lastovo plays an important role in local ecosystems, understanding the changes in driving mechanisms is of utmost importance for local biodiversity and socioeconomic status.

The low nutrient concentrations observed in 2022 are typical for the South Adriatic Sea [45,46], and the area around Lastovo Island is limited by phosphorus, which agrees with previous studies on this oligotrophic ecosystem (Matek et al. [19] and references therein). However, during our surveys of thermohaline oscillations in 2021 and 2022, we detected periods of enhanced nutrient concentrations (Matek et al. [19] and the present study), which correspond to the values reported for eutrophic systems in the Adriatic Sea [46–48]. This indicates a nutrient supply from the subsurface layer to the euphotic layer. Because these events coincided with strong diurnal thermocline dynamics forced by ITW events, we showed that diurnal thermocline dynamics under stratified conditions supply nutrients to the euphotic layer. The diurnal resonance has been recorded as important for nutrient fluxes driven by mixing and for enhanced phytoplankton productivity around a latitude of 30°S, where diurnal wind variability forces energetic inertial currents [49]. This is in accordance with previous research, where nutrient advection [50,51] and upwelling [52] have been recognized as crucial processes involving internal waves that impact primary production. In our study, there were no significant differences in nutrient concentrations in the water column during and after the ITW event, but the maximum phosphate concentrations in the thermocline

layer during the ITW event, as well as the significantly higher NPP in the same layer, may indicate possible nutrient support for the NPP.

Primary production in the Adriatic Sea is limited by phosphorus [21]; thus, the influx of phosphate to the surface layers can increase picoplankton primary production during periods of summer stratification [53,54] and may counteract the decline in primary production due to the increase in sea surface temperature caused by climate change [55]. Diel cycle variability in biogeochemical parameters arises from the competition between persistent grazing losses and respiration with daytime gross primary production [56]. A sinusoidal model that simulates this pattern can reproduce this relationship in oxygen measurements using glider profiles [33], drifting arrays [32], and moored bioptical observations [57]. To calculate the NPP and discuss its possible dynamics in relation to the ITW phenomenon, we used oxygen data measured using a high-resolution CTD probe. The enhanced NPP response during the ITW phenomena recorded in the thermocline layer may be due to the vertical diel DCM displacement. Neutrally buoyant phytoplankton cells are usually passive and can be significantly displaced vertically due to density fluctuations. In the region of Nazaré Canyon, west of Portugal, continuous passive motion of phytoplankton cells due to internal waves over a 3–4 days period resulted in an enhancement of photosynthesis [58]. The impact of internal waves on productivity has been reported in a lake ecosystem with up to 200 % higher photosynthesis [59] and a mean increase of 15 % in productivity in the deep open South China Sea [60]. Moreover, a recent idealized modeling study revealed an intensification of primary production along the internal tidal beams [61]. The reasons for this are twofold: (i) the larger local vertical displacement of water parcels, thereby reducing subsurface light limitation, and (ii) the convergence of nutrient flux in tidal beams, which leads to an enhancement of nutrient availability in the euphotic zone. Jacobsen et al. [61] concluded that, for internal tides, the effect of increased nutrient supply has a larger impact on primary production.

4.2. Phytoplankton distribution and variations in response to ITW events

The spatial and temporal distributions of phytoplankton and their correlations with environmental data agreed with observations from a recent study at the same location [19]. Although there was an evident response in the bacterial community diversity to ITW events, we observed no change in their abundance. Furthermore, ITWs did not influence the diversity or abundance of the eukaryotic communities. Picoplankton variability was mostly explained by temperature and nutrient concentrations as was previously reported for the Adriatic [62–65]. The separation of cyanobacterial taxa driven by nutrients, especially phosphate, has been reported in phosphorus-limited ecosystems [66]. *Synechococcus* is well adapted to a wide range of temperatures and nutrient concentrations [67,68], which may explain its dominance in the surface and thermocline layers.

The time lag in response to ITWs and the drivers behind this effect indicates that both light irradiance and nutrient supply play roles in the effects of ITWs on phytoplankton [69,70]. Specifically, increased exposure to light resulted in a rapid response in the smallest fractions composed of haptophytes, prasinophytes, and cryptophytes, whereas their reaction to nutrients was delayed by 12 h. This is in agreement with the results of our study, in which the response was recorded only in bacterioplankton. Conversely, diatoms benefited the most from an increase in light irradiance, exhibiting a response 12–16 h after ITWs [70]. Additionally, *Prochlorococcus* did not increase as it could not compete for enhanced nutrient concentrations and did not adapt to high light conditions, supporting our observation that *Prochlorococcus* was most adapted to the deep layer. Furthermore, research conducted in the South China Sea on the impact of internal solitary waves on plankton functionality has shown a shift from mixotrophic to autotrophic and heterotrophic plankton, especially small-scale diatoms and dinoflagellates, owing to nutrient advection [71]. Compared to similar research conducted recently in the South China Sea [70–72], the significance of our data lies in the high-resolution time-series data, offering insights into the succession of both prokaryotic and eukaryotic plankton communities during the ITW and non-ITW periods. Research on the impact of ITW on marine ecosystems is recent, but it has strong implications for understanding the adaptive strategies of plankton communities, especially primary producers, in stratified systems that will become more widespread and pronounced owing to climate change-induced sea surface temperatures.

Heterotrophic bacteria and PPEs showed a strong positive correlation with temperature, which is in agreement with other studies in the South Adriatic [73] and Mediterranean Seas [74], confirming that temperature increases and stratification affect the picoplankton community. Distinct spatial nano- and micro-phytoplankton distribution patterns in the stratified water column have been reported in the South Adriatic [62,75] and Mediterranean Sea [74] owing to different temperature optima [46] and distinct sinking rates of nano- and micro-fraction groups [76].

4.3. Zooplankton and bacterioplankton variations in response to ITW events

High-throughput sequencing (HTS) of marine ecosystems through methods such as environmental DNA (eDNA) metabarcoding is used to assess microbiome diversity and address the huge underexplored phylogenetic diversity of many new lineages [77]. Additionally, eDNA metabarcoding allows the estimation of the ecological significance of an investigated area using an interdisciplinary approach when coupled with physicochemical and bio-optical parameters [76,78]. Bacterioplankton communities regulate energy and matter fluxes and are fundamental to all higher trophic states, resulting in rapid bacterial responses to changes in dynamic environments. We observed bacterioplankton associations with unique physical forcing and oscillations in the thermocline and nutrients during an ITW event, in agreement with observations in the Baltic Sea, where environmental disturbances, phytoplankton succession, and salinity gradients shaped bacterioplankton communities [79]. Additionally, bacterioplankton and PPE abundances and compositions agree with other ultra-oligotrophic areas, such as the Eastern Mediterranean Sea [80], Indian Ocean [81], and South Adriatic Sea [26,27]. In general, fast bacterioplankton responses to physical forcing can be partly corroborated by investigations in the southern Adriatic Sea, explaining that bacteria, along with picoplankton, are pioneers in responding to convection, mixing events, or nutrient

fluxes on a fine scale [27,82,83]. However, this approach to studying bacterioplankton associated with grazer communities provides new insights.

Comprehensive sampling over two weeks resulting in 19 eDNA samples, and sampling with Nansen nets, ensuring high DNA yield for both gene markers, allowed us to use metabarcoding to answer questions about shifts in community composition during physical phenomena and subsequently to describe their putative ecological roles in such an environment. Although studies have relied on metagenome shotgun sequencing in searches for taxa shifts or metabolic pathways corresponding to certain environmental conditions [84,85], our applied approach of assessing communities with a combination of robust Aitchison distance in diversity analysis and FAPROTAX in functionality analysis allowed a clear distinction between bacterioplankton communities before and during the ITW event. The highly abundant copiotrophic Gammaproteobacteria relative to the more oligotrophic Alphaproteobacteria observed in this study are related to disturbances in stratified coastal oligotrophic conditions, such as those in the South Pacific Gyre along the Hawaii coast during heavy subtropical storm periods [86] or during convective mixing in the South Adriatic or Eastern Mediterranean Sea [27, 82,87]. Nevertheless, this dominance of Gammaproteobacteria over Alphaproteobacteria can partly be explained by the methodology of sampling (net tows instead of Niskin bottles), the prevalence of zooplankton-associated bacteria, and bacteria enhanced in abundance due to anthropogenic influences from the island. Furthermore, as studies have investigated bacterial communities from the perspective of human health and the preservation of marine areas, potentially industrial areas, and economically important areas (aquaculture) [88–90], we examined potential pathogens more closely. The fact that most bacteria shaping the community can be characterized as potentially pathogenic (Campylobacterales, *Pseudomonas*, *Pseudoalteromonas*, *Vibrio*) suggests that most of these bacteria are not just free-living in the water column, but also colonize zooplankton cells (attached to their exoskeleton) or live within their gut microbiome [91]. *Vibrio*, one of the most common and investigated zooplankton-associated pathogens, is a gram-negative bacterium that attaches to chitinous organisms, such as copepods, and grows within self-produced biofilms [92]. Additionally, *Vibrio* populations are influenced by environmental shifts, mostly in temperature and salinity [93]. *Pseudomonas*, *Pseudoalteromonas,* and *Alteromonas* were also found to be zooplankton-associated and in high proportion with respect to the whole bacterial community [94]. They were also identified as degraders, depleting oxygen concentrations [95]. Additionally, as De Corte et al. [96] showed, in calanoid and cyclopoid zooplankton communities, groups of Firmicutes (Bacillales, Lactobacillales, and Clostridiales), Actinobacteria (Actinomycetales), Fusobacteriales (*Fusobacterium* and *Leptotrichia*), *Alteromonas* and *Pseudomonas* from Gammaproteobacteria were exclusively associated with zooplankton net-towed samples rather than observations in the surrounding water [96]. Nevertheless, this study's limitation of the metabarcoding approach and the use of robust taxonomic assignment via the PR2 and QIIME2 platforms (~32, 000 citations so far) for amplicon analysis lies in the unrevealed metabolic associations of bacterial and zooplankton cells [84] and should serve as a baseline for future metagenomic studies in the South Adriatic Sea. Taxonomical assignment relying on one marker gene (in both cases, variable V4 regions) proved to be a common methodology for quick and correct identification [97], but could also be limiting for taxa that are phylogenetically highly diverse or still underappreciated [98]. Additionally, since this study aimed to detect these associations and community shifts at one seasonal point in time (summer stratification) over an intensive two-week sampling experiment, one cannot assess the seasonality of these associations, and future studies should investigate this.

The ecological functional roles of bacterioplankton described here match many of the traits of Gammaproteobacteria (especially *Alteromonas*, *Pseudoalteromonas,* and *Pseudomonas*), which are prominent marine microbial organisms that perform aerobic degradation of particulate organic matter [95]. Chemoheterotrophs, as the most dominant functional group observed during our experiment, reflect the dominance of facultative anaerobic bacteria, similarly found in environments with an enhanced organic matter load, anthropogenic influence, or bacterial communities associated with specific organisms, such as jellyfish [89,90,99]. Furthermore, crustacean zooplankton are responsible for releasing significant amounts of particulate organic matter and are dominant in abundance in ASVs; therefore, it is likely that most of the bacteria found were zooplankton-associated and mediated specific biogeochemical processes [84]. The observed bacterial composition and functional characteristics were similar to those observed in a study of marine wracks washed off Lastovo Island beaches by Kolda et al. (submitted) [100]. They analyzed data from Uska Bay on the island of Lastovo, which has the same exposure as the Struga station, with a beach impacted by high plastic debris loads, as occurs in other South Adriatic islands [101]. Samples collected from the beach in Uska Bay had a higher abundance of functional groups with the same bacterial activity as those detected in the sample collected at the end of the first ITW event (July 15, 2022). This may indicate high microplastic pollution in the water column and a possible negative effect of ITWs on microplastic resuspension from the sediment. Rhodobacteriaceae were also recorded in seagrass/plastic samples from the beach wreck and had higher abundances in the water column at the end of the second ITW event (July 15, 2022). Uska station also had the highest percentage of Vibrionales (up to 21.26 %) [100], which is characterized as an opportunistic pathogen and the first colonizer of plastic biofilms [102,103].

The composition and abundance of zooplankton communities revealed by traditional morphology-based approaches are characteristic of the oligotrophic coastal areas of the southern Adriatic Sea [104,105]. The microfraction is dominated by neritic tintinnids with a small number of deep-sea species and various nauplii and copepodites [106], whereas the composition of mesozooplankton is represented by nearshore species that also dominate the surface layer (up to 100 m) of the open sea [107]. The overall community composition based on HTS data showed similarities with a previous study by Stefanni et al. [108], which identified *Temora stylifera*, *Oithona similis*, *Paracalanus parvus parvus,* and various species from the genera *Calocalanus* and *Clausocalanus* along the Italian coast of the South Adriatic Sea. They also detected *Oncaea scottodicarloi*, *Acartia clausii*, *Mesocalanus tenuicornis*, *Nannocalanus minor,* and *Pseudocalanus moultoni* (for which the authors presumed that they were misidentified) that were not detected in this study from reads generated from the 18S rRNA gene, highlighting the importance of using the mitochondrial gene marker COI in identifying some zooplankton taxa [108]. Among the dominant copepods, appendicularians, and cladocerans in mesozooplankton, we detected unusually high abundances of nauplii and fish eggs, particularly at the end of the first ITW event (July 15, 2022).

Because of the high-resolution sampling design followed by fine-scale physicochemical changes, mesozooplankton grazers showed

daily shifts in the dominant taxa within the versatile community, following trends in NPP and overall phytoplankton and bacterioplankton succession according to their feeding preferences, which can be explained by mesozooplankton feeding preferences and changes in the phytoplankton community. For example, *C. typicus* showed higher abundance during ITW events (especially on the second and third days of the event) when the water column was dominated by nanoscale dinoflagellates, a motile prey that was shown in both natural and laboratory conditions to be its preferred prey under moderate to enhanced turbulence intensities [109]. On the other hand, the cladoceran *Evadne* sp. dominated at the end of both ITW events, thus altering to calanoid copepods, suggesting its opportunistic filter-feeding nature, preferring detritus and smaller pico-fractions, but also its ability to catch larger animal prey and graze on it [109]. Similar research has been conducted on other small copepods vs. cladoceran dietary niche overlap [110], which is consistent with our results. *Parvocalanus crassirostris* grazes predominantly on dinoflagellates, *Penilia avirostris* grazes primarily on diatoms and cnidarians, and *Pseudevadne tergestina* grazes on small crustaceans [110]. The dominance of the cyclopoid copepods *Oithona*, *Oncaea,* and *Corycaeus* after ITW events suggests grazing on residual microphytoplankton (mainly diatoms, *Oithona* and *Oncaea*), nanophytoplankton (mainly coccolithophorids, *Corycaeus*), and copepod nauplii (*Oithona* and *Oncaea*) [111,112]. However, because of the specific diet of nauplii and copepodites (mostly bacteria, picophytoplankton, small flagellates, and coccolithophorids), which are twenty times more abundant than fully developed calanoid and cyclopoid copepods, we hypothesized that *Oithona* bloom in periods without strong ITW forcing was the exact consequence of this imbalance [111,112].

5. Conclusions

Our study confirmed the recurring occurrence of large but intermittent diurnal internal island-trapped waves around Lastovo Island during periods with a stratified water column. Their range is highly dependent on background thermohaline properties and physical forcing. The results indicated that Lastovo is an ideal environment for physicochemical and biological experiments, particularly when research is coupled with operational meteo-oceanographic forecasts, enabling more adaptive and efficient sampling.

The use of operational atmospheric and oceanographic models allowed the prediction of intense ITW episodes and the rapid adaptation of fieldwork, with four times per day sampling during intense ITW events. This sampling demonstrated that ITW episodes coincided with elevated NPP in the thermocline layer, where enhanced phosphate concentrations were also detected. There was no observed response in the community structure or abundance of the eukaryotic plankton community.

Bacterioplankton responded to ITW episodes in terms of their composition and ecological functions. Most bacterial functions represented degradation processes or processes associated with elevated NPP. Functional groups were equally distributed during the study period, with a slightly increased abundance during ITW events. The grazer-decomposer point of view highlights the importance of the heterotrophic fraction of plankton, while primary production depends on pico-sized cells that are eaten very quickly, thus generating short but intensive NPP fluxes.

We applied an adaptive sampling strategy to obtain a unique dataset of physicochemical and bio-optical parameters. Combined with eDNA metabarcoding techniques, this represents a thorough interdisciplinary approach applicable to similar sites where island masses affect physical and biological processes. This study showed a biological response to ITW events in the South Adriatic; however, the main mechanisms of either nutrient- or light-driven processes remain to be elucidated. Because water column stratification is increasing due to climate change, the importance of defining primary production hotspots is imperative for future research and environmental management.

Data availability statement

A PUH data storage and management service publication page was established (https://puh.srce.hr/s/ZSS2qz8ji5PStDj) with scripts, code snippets, and raw data used in this study. They are available upon request, as described in the PUH publication web page. Raw sequences of eDNA were deposited in the European Nucleotide Archive (ENA) under project number PRJEB63220.

CRediT authorship contribution statement

Zrinka Ljubešić: Writing – review & editing, Writing – original draft, Supervision, Resources, Project administration, Methodology, Investigation, Funding acquisition, Formal analysis, Data curation, Conceptualization. **Hrvoje Mihanović:** Writing – review & editing, Writing – original draft, Visualization, Validation, Supervision, Software, Methodology, Investigation, Funding acquisition, Formal analysis, Data curation, Conceptualization. **Antonija Matek:** Writing – review & editing, Writing – original draft, Visualization, Project administration, Investigation, Data curation. **Maja Mucko:** Writing – review & editing, Writing – original draft, Visualization, Methodology, Investigation, Formal analysis, Data curation. **Eric P. Achterberg:** Writing – review & editing, Resources, Investigation, Formal analysis. **Melissa Omand:** Writing – review & editing, Visualization, Validation, Supervision, Software, Resources, Methodology, Investigation, Funding acquisition, Formal analysis. **Branka Pestorić:** Writing – review & editing, Resources, Investigation, Formal analysis. **Davor Lučić:** Writing – review & editing, Investigation, Formal analysis. **Hrvoje Čižmek:** Writing – review & editing, Methodology, Investigation. **Barbara Čolić:** Writing – review & editing, Methodology, Investigation. **Cecilia Balestra:** Writing – review & editing, Formal analysis. **Raffaella Casotti:** Writing – review & editing, Resources. **Ivica Janeković:** Writing – review & editing, Validation, Software, Methodology. **Mirko Orlić:** Writing – review & editing, Validation, Supervision, Methodology, Investigation.

Declaration of competing interest

The authors declare that they have no known competing financial interests or personal relationships that could have appeared to influence the work reported in this paper.

Acknowledgements

This work was fully funded by the Croatian Science Foundation under the ISLAND project (IP-2020-02-9524). Antonija Matek has been funded by the Croatian Science Foundation under the "Young Researchers' Career Development Project - Training New Doctoral Students". Wind data from the Lastovo meteorological station were provided by the Croatian Meteorological and Hydrological Service (DHMZ). We thank the captain and crew of the R/V *Baldo Kosić II*, Marine Explorers Society 20.000 leagues team, Rade Garić, Marcel Denes, and Dobroslav Jukić, who made this research possible.

Appendix A. Supplementary data

Supplementary data to this article can be found online at https://doi.org/10.1016/j.heliyon.2024.e37788.

References

[1] C.B. Field, M.J. Behrenfeld, J.T. Randerson, P. Falkowski, Primary production of the biosphere: integrating terrestrial and oceanic components, Science 281 (1998) 237–240, https://doi.org/10.1126/science.281.5374.237.
[2] D.W. Fahey, S.J. Doherty, K.A. Hibbard, A. Romanou, P.C. Taylor, D.J. Wuebbles, D.W. Fahey, K.A. Hibbard, D.J. Dokken, B.C. Stewart, T.K. Maycock, Chapter 2: physical drivers of climate change, in: Climate Science Special Report: A Sustained Assessment Activity of the U.S. Global Change Research Program, U.S. Global Change Research Program, Washington, DC, USA, 2017, https://doi.org/10.7930/J0513WCR.
[3] M.S. Doty, M. Oguri, The island mass effect, ICES (Int. Counc. Explor. Sea) J. Mar. Sci. 22 (1956) 33–37, https://doi.org/10.1093/icesjms/22.1.33.
[4] J.M. Gove, M.A. McManus, A.B. Neuheimer, J.J. Polovina, J.C. Drazen, C.R. Smith, M.A. Merrifield, A.M. Friedlander, J.S. Ehses, C.W. Young, A.K. Dillon, G. J. Williams, Near-island biological hotspots in barren ocean basins, Nat. Commun. 7 (2016) 10581, https://doi.org/10.1038/ncomms10581.
[5] C. De Falco, F. Desbiolles, A. Bracco, C. Pasquero, Island mass effect: a review of oceanic physical processes, Front. Mar. Sci. 9 (2022) 894860, https://doi.org/10.3389/fmars.2022.894860.
[6] N.G. Hogg, Observations of internal kelvin waves trapped round Bermuda, J. Phys. Oceanogr. 10 (1980) 1353–1376, https://doi.org/10.1175/1520-0485(1980)010<1353:OOIKWT>2.0.CO;2.
[7] K.H. Brink, Island-trapped waves, with application to observations off Bermuda, Dynam. Atmos. Oceans 29 (1999) 93–118, https://doi.org/10.1016/S0377-0265(99)00003-2.
[8] D.S. Luther, Trapped waves around the Hawaiian Islands, in: Hawaiian Ocean Experiment: Proc. 3rd 'Aha Huliko 'a Hawaiian Winter Workshop, 1985, pp. 261–301. Honolulu, HI, USA.
[9] M.A. Merrifield, L. Yang, D.S. Luther, Numerical simulations of a storm-generated island-trapped wave event at the Hawaiian Islands, J. Geophys. Res.: Oceans 107 (2002), https://doi.org/10.1029/2001JC001134, 33-1-33–10.
[10] K.A. Smith, M.A. Merrifield, G.S. Carter, Coastal-trapped behavior of the diurnal internal tide at O 'ahu, H awai'i, JGR Oceans 122 (2017) 4257–4273, https://doi.org/10.1002/2016JC012436.
[11] O. Pizarro, G. Shaffer, Wind-driven, coastal-trapped waves off the island of Gotland, Baltic Sea, J. Phys. Oceanogr. 28 (1998) 2117–2129, https://doi.org/10.1175/1520-0485(1998)028<2117:WDCTWO>2.0.CO;2.
[12] A. Jordi, G. Basterretxea, D.-P. Wang, Evidence of sediment resuspension by island trapped waves, Geophys. Res. Lett. 36 (2009), https://doi.org/10.1029/2009GL040055.
[13] H. Mihanović, M. Orlić, Z. Pasarić, Diurnal thermocline oscillations driven by tidal flow around an island in the Middle Adriatic, J. Mar. Syst. 78 (2009) S157–S168, https://doi.org/10.1016/j.jmarsys.2009.01.021.
[14] M. Orlić, G. Beg Paklar, V. Dadić, N. Leder, H. Mihanović, M. Pasarić, Z. Pasarić, Diurnal upwelling resonantly driven by sea breezes around an Adriatic island, J. Geophys. Res. 116 (2011) C09025, https://doi.org/10.1029/2011JC006955.
[15] P. Lazure, B. Le Cann, M. Bezaud, Large diurnal bottom temperature oscillations around the Saint Pierre and Miquelon archipelago, Sci. Rep. 8 (2018) 13882, https://doi.org/10.1038/s41598-018-31857-w.
[16] M. Novosel, A. Požar-Domac, M. Pasarić, Diversity and distribution of the bryozoa along underwater cliffs in the Adriatic Sea with special reference to thermal regime, Mar. Ecol. 25 (2004) 155–170, https://doi.org/10.1111/j.1439-0485.2004.00022.x.
[17] H. Mihanović, M. Orlić, Z. Pasarić, Diurnal internal tides detected in the Adriatic, Ann. Geophys. 24 (2006) 2773–2780, https://doi.org/10.5194/angeo-24-2773-2006.
[18] V. Artale, A. Provenzale, R. Santoleri, Analysis of internal temperature oscillations of tidal period on the Sicilian continental shelf, in: Continental Shelf Research, 1989, pp. 867–888, https://doi.org/10.1016/0278-4343(89)90063-0.
[19] A. Matek, M. Mucko, R. Casotti, A. Trano, E. Achterberg, H. Mihanović, H. Cizmek, B. Čolić, V. Cuculić, Z. Ljubesic, Phytoplankton diversity and co-dependency in a stratified oligotrophic ecosystem in the South Adriatic Sea, Water 15 (2023) 2299, https://doi.org/10.3390/w15122299.
[20] M. Turchetto, F. Bianchi, A. Boldrin, A. Malaguti, S. Rabitti, G. Socal, L. Strada, Nutrients, phytoplankton and primary production processes in oligotrophic areas (Southern Adriatic and Northern Ionian), Atti AIOL 13 (2000) 269–278.
[21] I. Marasović, Ž. Ninčević, G. Kušpilić, S. Marinović, S. Marinov, Long-term changes of basic biological and chemical parameters at two stations in the middle Adriatic, J. Sea Res. 54 (2005) 3–14, https://doi.org/10.1016/j.seares.2005.02.007.
[22] A. Pugnetti, F. Acri, L. Alberighi, D. Barletta, M. Bastianini, F. Bernardi-Aubry, A. Berton, F. Bianchi, G. Socal, C. Totti, Phytoplankton photosynthetic activity and growth rates in the NW Adriatic Sea, Chem. Ecol. 20 (2004) 399–409, https://doi.org/10.1080/02757540412331294902.
[23] B. Grbec, M. Morović, G.B. Paklar, G. Kušpilić, S. Matijević, F. Matić, Ž.N. Gladan, The relationship between the atmospheric variability and productivity in the Adriatic Sea area, J. Mar. Biol. Assoc. U. K. 89 (2009) 1549–1558, https://doi.org/10.1017/S0025315409000708.
[24] G. Civitarese, M. Gačić, M. Lipizer, G.L. Eusebi Borzelli, On the impact of the bimodal oscillating system (BiOS) on the biogeochemistry and biology of the adriatic and ionian seas (eastern mediterranean), Biogeosciences 7 (2010) 3987–3997, https://doi.org/10.5194/bg-7-3987-2010.
[25] I. Marasović, D. Viličić, Ž. Ninčević, South adriatic ecosystem: interaction with the Mediterranean Sea, in: P. Malanotte-Rizzoli, V.N. Eremeev (Eds.), The Eastern Mediterranean as a Laboratory Basin for the Assessment of Contrasting Ecosystems, Springer Netherlands, Dordrecht, 1999, pp. 383–405, https://doi.org/10.1007/978-94-011-4796-5_25.

[26] M. Mucko, S. Bosak, R. Casotti, C. Balestra, Z. Ljubešić, Winter picoplankton diversity in an oligotrophic marginal sea, Mar. Genomics 42 (2018) 14–24, https://doi.org/10.1016/j.margen.2018.09.002.

[27] I. Babić, M. Mucko, I. Petrić, S. Bosak, H. Mihanović, I. Vilibić, I. Dupčić Radić, I. Cetinić, C. Balestra, R. Casotti, Z. Ljubešić, Multilayer approach for characterization of bacterial diversity in a marginal sea: from surface to seabed, J. Mar. Syst. 184 (2018) 15–27, https://doi.org/10.1016/j.jmarsys.2018.04.002.

[28] A.F. Shchepetkin, J.C. McWilliams, The regional oceanic modeling system (ROMS): a split-explicit, free-surface, topography-following-coordinate oceanic model, Ocean Model. 9 (2005) 347–404, https://doi.org/10.1016/j.ocemod.2004.08.002.

[29] A.F. Shchepetkin, J.C. McWilliams, Correction and commentary for "Ocean forecasting in terrain-following coordinates: Formulation and skill assessment of the regional ocean modeling system" by Haidvogel et al., J. Comp. Phys. 227, pp. 3595–3624., Journal of Computational Physics 228 (2009) 8985–9000. https://doi.org/10.1016/j.jcp.2009.09.002.

[30] I. Janeković, H. Mihanović, I. Vilibić, B. Grčić, S. Ivatek-Šahdan, M. Tudor, T. Djakovac, Using multi-platform 4D-Var data assimilation to improve modeling of Adriatic Sea dynamics, Ocean Model. 146 (2020) 101538, https://doi.org/10.1016/j.ocemod.2019.101538.

[31] R. Harris, P. Wiebe, J. Lenz, H.R. Skjoldal, M. Huntley, ICES Zooplankton Methodology Manual, Elsevier, Academic Press, London, 2000, https://doi.org/10.1016/B978-0-12-327645-2.X5000-2.

[32] B. Barone, D. Nicholson, S. Ferrón, E. Firing, D. Karl, The estimation of gross oxygen production and community respiration from autonomous time-series measurements in the oligotrophic ocean, Limnol Oceanogr. Methods 17 (2019) 650–664, https://doi.org/10.1002/lom3.10340.

[33] D.P. Nicholson, S.T. Wilson, S.C. Doney, D.M. Karl, Quantifying subtropical North Pacific gyre mixed layer primary productivity from Seaglider observations of diel oxygen cycles, Geophys. Res. Lett. 42 (2015) 4032–4039, https://doi.org/10.1002/2015GL063065.

[34] S. Andrews, Babraham bioinformatics - FastQC A quality control tool for high throughput sequence data. https://www.bioinformatics.babraham.ac.uk/projects/fastqc/, 2010. (Accessed 5 December 2022).

[35] P. Ewels, M. Magnusson, S. Lundin, M. Käller, MultiQC: summarize analysis results for multiple tools and samples in a single report, Bioinformatics 32 (2016) 3047–3048, https://doi.org/10.1093/bioinformatics/btw354.

[36] E. Bolyen, J.R. Rideout, M.R. Dillon, N.A. Bokulich, C.C. Abnet, G.A. Al-Ghalith, H. Alexander, E.J. Alm, M. Arumugam, F. Asnicar, Y. Bai, J.E. Bisanz, K. Bittinger, A. Brejnrod, C.J. Brislawn, C.T. Brown, B.J. Callahan, A.M. Caraballo-Rodríguez, J. Chase, E.K. Cope, R. Da Silva, C. Diener, P.C. Dorrestein, G. M. Douglas, D.M. Durall, C. Duvallet, C.F. Edwardson, M. Ernst, M. Estaki, J. Fouquier, J.M. Gauglitz, S.M. Gibbons, D.L. Gibson, A. Gonzalez, K. Gorlick, J. Guo, B. Hillmann, S. Holmes, H. Holste, C. Huttenhower, G.A. Huttley, S. Janssen, A.K. Jarmusch, L. Jiang, B.D. Kaehler, K.B. Kang, C.R. Keefe, P. Keim, S. T. Kelley, D. Knights, I. Koester, T. Kosciolek, J. Kreps, M.G.I. Langille, J. Lee, R. Ley, Y.-X. Liu, E. Loftfield, C. Lozupone, M. Maher, C. Marotz, B.D. Martin, D. McDonald, L.J. McIver, A.V. Melnik, J.L. Metcalf, S.C. Morgan, J.T. Morton, A.T. Naimey, J.A. Navas-Molina, L.F. Nothias, S.B. Orchanian, T. Pearson, S. L. Peoples, D. Petras, M.L. Preuss, E. Pruesse, L.B. Rasmussen, A. Rivers, M.S. nd Robeson, P. Rosenthal, N. Segata, M. Shaffer, A. Shiffer, R. Sinha, S.J. Song, J. R. Spear, A.D. Swafford, L.R. Thompson, P.J. Torres, P. Trinh, A. Tripathi, P.J. Turnbaugh, S. Ul-Hasan, J.J.J. van der Hooft, F. Vargas, Y. Vázquez-Baeza, E. Vogtmann, M. von Hippel, W. Walters, Y. Wan, M. Wang, J. Warren, K.C. Weber, C.H.D. Williamson, A.D. Willis, Z.Z. Xu, J.R. Zaneveld, Y. Zhang, Q. Zhu, R. Knight, J.G. Caporaso, Reproducible, interactive, scalable and extensible microbiome data science using QIIME 2, Nat. Biotechnol. 37 (2019) 852–857, https://doi.org/10.1038/s41587-019-0209-9.

[37] B.J. Callahan, P.J. McMurdie, M.J. Rosen, A.W. Han, A.J.A. Johnson, S.P. Holmes, DADA2: high-resolution sample inference from Illumina amplicon data, Nat. Methods 13 (2016) 581–583, https://doi.org/10.1038/nmeth.3869.

[38] C. Quast, E. Pruesse, P. Yilmaz, J. Gerken, T. Schweer, P. Yarza, J. Peplies, F.O. Glöckner, The SILVA ribosomal RNA gene database project: improved data processing and web-based tools, Nucleic Acids Res. 41 (2013) D590–D596, https://doi.org/10.1093/nar/gks1219.

[39] L. Guillou, D. Bachar, S. Audic, D. Bass, C. Berney, L. Bittner, C. Boutte, G. Burgaud, C. de Vargas, J. Decelle, J. del Campo, J.R. Dolan, M. Dunthorn, B. Edvardsen, M. Holzmann, W.H.C.F. Kooistra, E. Lara, N. Le Bescot, R. Logares, F. Mahé, R. Massana, M. Montresor, R. Morard, F. Not, J. Pawlowski, I. Probert, A.-L. Sauvadet, R. Siano, T. Stoeck, D. Vaulot, P. Zimmermann, R. Christen, The Protist Ribosomal Reference database (PR2): a catalog of unicellular eukaryote Small Sub-Unit rRNA sequences with curated taxonomy, Nucleic Acids Res. 41 (2013) D597–D604, https://doi.org/10.1093/nar/gks1160.

[40] C. Martino, J.T. Morton, C.A. Marotz, L.R. Thompson, A. Tripathi, R. Knight, K. Zengler, A novel sparse compositional technique reveals microbial perturbations, mSystems 4 (2019), https://doi.org/10.1128/msystems.00016-19.

[41] M.W. Fedarko, C. Martino, J.T. Morton, A. González, G. Rahman, C.A. Marotz, J.J. Minich, E.E. Allen, R. Knight, Visualizing 'omic feature rankings and log-ratios using Qurro, NAR Genomics and Bioinformatics 2 (2020), https://doi.org/10.1093/nargab/lqaa023 lqaa023.

[42] S. Louca, L.W. Parfrey, M. Doebeli, Decoupling function and taxonomy in the global ocean microbiome, Science 353 (2016) 1272–1277, https://doi.org/10.1126/science.aaf4507.

[43] H. Mihanović, G. Beg Paklar, M. Orlić, Resonant excitation of island-trapped waves in a shallow, seasonally stratified sea, Continent. Shelf Res. 77 (2014) 24–37, https://doi.org/10.1016/j.csr.2014.01.014.

[44] Croatian Meteorological and Hydrological Service. Meteorological and hydrological bulletin 7/2022 (in Croatian), 2022, p. 58. Zagreb, Croatia.

[45] D. Viličić, Z. Vučak, A. Škrivanić, Z. Gržetić, Phytoplankton blooms in the oligotrophic open south Adriatic Waters, Mar. Chem. 28 (1989) 89–107, https://doi.org/10.1016/0304-4203(89)90189-8.

[46] D. Viličić, Phytoplankton taxonomy and distribution in the offshore southern Adriatic, Nat. Croat. 7 (1998) 127–141.

[47] D. Drakulović, S. Krivokapić, M. Mandić, A. Redžic, Phytoplankton community in boka kotorska bay (South-Eastern adriatic), Rapp. Comm. Int. Mer Médit. 40 (2013) 428.

[48] N. Jasprica, M. Čalić, V. Kovačević, M. Bensi, I. Dupčić Radić, R. Garić, M. Batistić, Phytoplankton distribution related to different winter conditions in 2016 and 2017 in the open southern Adriatic Sea (eastern Mediterranean), J. Mar. Syst. 226 (2022) 103665, https://doi.org/10.1016/j.jmarsys.2021.103665.

[49] A.J. Lucas, G.C. Pitcher, T.A. Probyn, R.M. Kudela, The influence of diurnal winds on phytoplankton dynamics in a coastal upwelling system off southwestern Africa, Deep Sea Res. Part II Top. Stud. Oceanogr. 101 (2014) 50–62, https://doi.org/10.1016/j.dsr2.2013.01.016.

[50] S. MacIntyre, R. Jellison, Nutrient fluxes from upwelling and enhanced turbulence at the top of the pycnocline in Mono Lake, California, Hydrobiologia 466 (2001) 13–29.

[51] P. Sangrà, G. Basterretxea, J.L. Pelegrí, J. Arístegui, Chlorophyll increase due to internal waves in the shelf-break of gran canaria island (canary islands), Sci. Mar. 65 (2001) 89–97, https://doi.org/10.3989/scimar.2001.65s189.

[52] J.M. Pringle, K. Riser, Remotely forced nearshore upwelling in Southern California, J. Geophys. Res.: Oceans 108 (2003), https://doi.org/10.1029/2002JC001447.

[53] N. Krstulović, T. Pucher-Petković, M. Šolić, The relation between bacterioplankton and phytoplankton production in the mid Adriatic Sea, Aquat. Microb. Ecol. 9 (1995) 41–45, https://doi.org/10.3354/ame009041.

[54] L. Ignatiades, S. Psarra, V. Zervakis, K. Pagou, E. Souvermezoglou, G. Assimakopoulou, O. Gotsis-Skretas, Phytoplankton size-based dynamics in the aegean sea (eastern mediterranean), J. Mar. Syst. 36 (2002) 11–28, https://doi.org/10.1016/S0924-7963(02)00132-X.

[55] J.K. Moore, W. Fu, F. Primeau, G.L. Britten, K. Lindsay, M. Long, S.C. Doney, N. Mahowald, F. Hoffman, J.T. Randerson, Sustained climate warming drives declining marine biological productivity, Science 359 (2018) 1139–1143, https://doi.org/10.1126/science.aao6379.

[56] J. Marra, Analysis of diel variability in chlorophyll fluorescence, J. Mar. Res. 55 (1997) 767–784.

[57] A.E. White, B. Barone, R.M. Letelier, D.M. Karl, Productivity diagnosed from the diel cycle of particulate carbon in the North Pacific Subtropical Gyre, Geophys. Res. Lett. 44 (2017) 3752–3760, https://doi.org/10.1002/2016GL071607.

[58] S. Muacho, J.C.B. da Silva, V. Brotas, P.B. Oliveira, Effect of internal waves on near-surface chlorophyll concentration and primary production in the Nazaré Canyon (west of the Iberian Peninsula), Deep Sea Res. Oceanogr. Res. Pap. 81 (2013) 89–96, https://doi.org/10.1016/j.dsr.2013.07.012.

[59] M.A. Evans, S. MacIntyre, G.W. Kling, Internal wave effects on photosynthesis: experiments, theory, and modeling, Limnol. Oceanogr. 53 (2008) 339–353, https://doi.org/10.4319/lo.2008.53.1.0339.

[60] X. Pan, G.T.F. Wong, F.-K. Shiah, T.-Y. Ho, Enhancement of biological productivity by internal waves: observations in the summertime in the northern South China Sea, J. Oceanogr. 68 (2012) 427–437, https://doi.org/10.1007/s10872-012-0107-y.

[61] J.R. Jacobsen, C.A. Edwards, B.S. Powell, J.A. Colosi, J. Fiechter, Nutricline adjustment by internal tidal beam generation enhances primary production in idealized numerical models, Front. Mar. Sci. 10 (2023) 1309011, https://doi.org/10.3389/fmars.2023.1309011.

[62] T. Šilović, Z. Ljubešić, H. Mihanović, G. Olujić, S. Terzić, Ž. Jakšić, D. Viličić, Picoplankton composition related to thermohaline circulation: the Albanian boundary zone (southern Adriatic) in late spring, Estuarine, Coastal and Shelf Science 91 (2011) 519–525, https://doi.org/10.1016/j.ecss.2010.12.012.

[63] D. Šantić, V. Kovačević, M. Bensi, M. Giani, A. Vrdoljak Tomaš, M. Ordulj, C. Santinelli, S. Šestanović, M. Šolić, B. Grbec, Picoplankton distribution and activity in the deep waters of the Southern Adriatic Sea, Water 11 (2019) 1655, https://doi.org/10.3390/w11081655.

[64] M. Šolić, D. Šantić, S. Šestanović, N. Bojanić, B. Grbec, S. Jozić, A. Vrdoljak, M. Ordulj, F. Matić, G. Kušpilić, Ž.N. Gladan, Impact of water column stability dynamics on the succession of plankton food web types in the offshore area of the Adriatic Sea, J. Sea Res. 158 (2020) 101860, https://doi.org/10.1016/j.seares.2020.101860.

[65] D. Šantić, I. Stojan, F. Matić, Ž. Trumbić, A. Vrdoljak Tomaš, Ž. Fredotović, K. Piwosz, I. Lepen Pleić, S. Šestanović, M. Šolić, Picoplankton diversity in an oligotrophic and high salinity environment in the central Adriatic Sea, Sci. Rep. 13 (2023) 7617, https://doi.org/10.1038/s41598-023-34704-9.

[66] M. Šolić, N. Krstulović, D. Šantić, S. Šestanović, M. Ordulj, N. Bojanić, G. Kuspilić, Structure of microbial communities in phosphorus-limited estuaries along the eastern Adriatic coast, J. Mar. Biol. Assoc. U. K. 95 (2015) 1565–1578, https://doi.org/10.1017/S0025315415000442.

[67] J. Pittera, F. Humily, M. Thorel, D. Grulois, L. Garczarek, C. Six, Connecting thermal physiology and latitudinal niche partitioning in marine Synechococcus, ISME J. 8 (2014) 1221–1236, https://doi.org/10.1038/ismej.2013.228.

[68] A. Coello-Camba, S. Agustí, Picophytoplankton niche partitioning in the warmest oligotrophic sea, Front. Mar. Sci. 8 (2021) 651877, https://doi.org/10.3389/fmars.2021.651877.

[69] Y.-H. Wang, C.-F. Dai, Y.-Y. Chen, Physical and ecological processes of internal waves on an isolated reef ecosystem in the South China Sea, Geophys. Res. Lett. 34 (2007), https://doi.org/10.1029/2007GL030658.

[70] L. Ma, W. Xiao, E.A. Laws, X. Bai, K.-P. Chiang, X. Liu, J. Chen, B. Huang, Responses of phytoplankton communities to the effect of internal wave-powered upwelling, Limnol. Oceanogr. 66 (2020) 1083–1098, https://doi.org/10.1002/lno.11666.

[71] Z. Guan, R. Ge, Y. Li, L. Zou, S. Yang, Diel variation of phytoplankton communities in the northern South China Sea under the effect of internal solitary waves and its response to environmental factors, Water 15 (2023) 2422, https://doi.org/10.3390/w15132422.

[72] L. Ma, X. Bai, E.A. Laws, W. Xiao, C. Guo, X. Liu, K.-P. Chiang, K. Gao, B. Huang, Responses of phytoplankton communities to internal waves in oligotrophic oceans, J. Geophys. Res.: Oceans 128 (2023) e2023JC020201, https://doi.org/10.1029/2023JC020201.

[73] D. Šantić, N. Krstulovic, M. Solic, G. Kušpilić, HNA and LNA bacteria in relation to the activity of heterotrophic bacteria, Acta Adriat. 53 (2012) 25–40.

[74] C. Mena, P. Reglero, M. Hidalgo, E. Sintes, R. Santiago, M. Martín, G. Moyà, R. Balbín, Phytoplankton community structure is driven by stratification in the oligotrophic Mediterranean Sea, Front. Microbiol. 10 (2019) 1698, https://doi.org/10.3389/fmicb.2019.01698.

[75] T. Šilović, H. Mihanović, M. Batistić, I.D. Radić, E. Hrustić, M. Najdek, Picoplankton distribution influenced by thermohaline circulation in the southern Adriatic, Continent. Shelf Res. 155 (2018) 21–33, https://doi.org/10.1016/j.csr.2018.01.007.

[76] C.A. Durkin, I. Cetinić, M. Estapa, Z. Ljubešić, M. Mucko, A. Neeley, M. Omand, Tracing the path of carbon export in the ocean though DNA sequencing of individual sinking particles, ISME J. 16 (2022) 1896–1906, https://doi.org/10.1038/s41396-022-01239-2.

[77] K.M. Ruppert, R.J. Kline, M.S. Rahman, Past, present, and future perspectives of environmental DNA (eDNA) metabarcoding: a systematic review in methods, monitoring, and applications of global eDNA, Global Ecology and Conservation 17 (2019) e00547, https://doi.org/10.1016/j.gecco.2019.e00547.

[78] L. MacNeil, D.K. Desai, M. Costa, J. LaRoche, Combining multi-marker metabarcoding and digital holography to describe eukaryotic plankton across the Newfoundland Shelf, Sci. Rep. 12 (2022) 1–11, https://doi.org/10.1038/s41598-022-17313-w.

[79] M.V. Lindh, J. Pinhassi, Sensitivity of bacterioplankton to environmental disturbance: a review of Baltic Sea field studies and experiments, Front. Mar. Sci. 5 (2018), https://doi.org/10.3389/fmars.2018.00361.

[80] T. Reich, T. Ben-Ezra, N. Belkin, A. Tsemel, D. Aharonovich, D. Roth-Rosenberg, S. Givati, M. Bialik, B. Herut, I. Berman-Frank, M. Frada, M.D. Krom, Y. Lehahn, E. Rahav, D. Sher, A year in the life of the Eastern Mediterranean: monthly dynamics of phytoplankton and bacterioplankton in an ultra-oligotrophic sea, Deep Sea Res. Oceanogr. Res. Pap. 182 (2022) 103720, https://doi.org/10.1016/j.dsr.2022.103720.

[81] J. Li, X. Liu, N. Xie, M. Bai, L. Liu, B. Sen, G. Wang, Subsurface bacterioplankton structure and diversity in the strongly-stratified water columns within the equatorial eastern Indian ocean, Microorganisms 11 (2023) 592, https://doi.org/10.3390/microorganisms11030592.

[82] M. Korlević, P. Pop Ristova, R. Garić, R. Amann, S. Orlić, Bacterial diversity in the South Adriatic Sea during a strong deep winter convection year, Appl. Environ. Microbiol. 81 (2015) 1715–1726, https://doi.org/10.1128/AEM.03410-14.

[83] M. Šolić, D. Šantić, S. Šestanović, G. Kušpilić, F. Matić, A. Vrdoljak Tomaš, S. Jozić, N. Bojanić, Ž. Ninčević Gladan, Changing ecological conditions in the marine environment generate different microbial food web structures in a repeatable manner, Front. Mar. Sci. 8 (2022), https://doi.org/10.3389/fmars.2021.811155.

[84] D. De Corte, A. Srivastava, M. Koski, J.A.L. Garcia, Y. Takaki, T. Yokokawa, T. Nunoura, N.H. Elisabeth, E. Sintes, G.J. Herndl, Metagenomic insights into zooplankton-associated bacterial communities, Environ. Microbiol. 20 (2018) 492–505, https://doi.org/10.1111/1462-2920.13944.

[85] F. Wang, S. Guo, J. Liang, X. Sun, Water column stratification governs picophytoplankton community structure in the oligotrophic eastern Indian ocean, Mar. Environ. Res. 189 (2023) 106074, https://doi.org/10.1016/j.marenvres.2023.106074.

[86] S.K. Yeo, M.J. Huggett, A. Eiler, M.S. Rappé, Coastal bacterioplankton community dynamics in response to a natural disturbance, PLoS One 8 (2013) e56207, https://doi.org/10.1371/journal.pone.0056207.

[87] M. Haber, D. Roth Rosenberg, M. Lalzar, I. Burgsdorf, K. Saurav, R. Lionheart, Y. Lehahn, D. Aharonovich, L. Gómez-Consarnau, D. Sher, M.D. Krom, L. Steindler, Spatiotemporal variation of microbial communities in the ultra-oligotrophic eastern Mediterranean Sea, Front. Microbiol. 13 (2022), https://doi.org/10.3389/fmicb.2022.867694.

[88] L.N. Duarte, F.J.R.C. Coelho, D.F.R. Cleary, D. Bonifácio, P. Martins, N.C.M. Gomes, Bacterial and microeukaryotic plankton communities in a semi-intensive aquaculture system of sea bass (*Dicentrarchus labrax*): a seasonal survey, Aquaculture 503 (2019) 59–69, https://doi.org/10.1016/j.aquaculture.2018.12.066.

[89] F. Sun, Y. Wang, C. Wang, L. Zhang, K. Tu, Z. Zheng, Insights into the intestinal microbiota of several aquatic organisms and association with the surrounding environment, Aquaculture 507 (2019) 196–202, https://doi.org/10.1016/j.aquaculture.2019.04.026.

[90] A. Kolda, A. Gavrilović, J. Jug-Dujaković, Z. Ljubešić, M. El-Matbouli, A. Lillehaug, S. Lončarević, L. Perić, D. Knežević, D. Vukić Lušić, D. Kapetanović, Profiling of bacterial assemblages in the marine cage farm environment, with implications on fish, human and ecosystem health, Ecol. Indicat. 118 (2020) 106785, https://doi.org/10.1016/j.ecolind.2020.106785.

[91] L. Vezzulli, R.R. Colwell, C. Pruzzo, Ocean warming and spread of pathogenic vibrios in the aquatic environment, Microb. Ecol. 65 (2013) 817–825, https://doi.org/10.1007/s00248-012-0163-2.

[92] G.C. De Magny, P.K. Mozumder, C.J. Grim, N.A. Hasan, M.N. Naser, M. Alam, R.B. Sack, A. Huq, R.R. Colwell, Role of zooplankton diversity in Vibrio cholerae population dynamics and in the incidence of cholera in the Bangladesh sundarbans, Appl. Environ. Microbiol. 77 (2011) 6125–6132, https://doi.org/10.1128/AEM.01472-10.

[93] A. Romero, M. del M. Costa, G. Forn-Cuni, P. Balseiro, R. Chamorro, S. Dios, A. Figueras, B. Novoa, Occurrence, seasonality and infectivity of Vibrio strains in natural populations of mussels Mytilus galloprovincialis, Dis. Aquat. Org. 108 (2014) 149–163, https://doi.org/10.3354/dao02701.

[94] K.E. Costello, D. Haberlin, S.A. Lynch, R. McAllen, R.M. O'Riordan, S.C. Culloty, Regional differences in zooplankton-associated bacterial communities and aquaculture pathogens across two shelf seas, Estuar. Coast Shelf Sci. 281 (2023) 108179, https://doi.org/10.1016/j.ecss.2022.108179.

[95] C. Henríquez-Castillo, A.M. Plominsky, S. Ramírez-Flandes, A.D. Bertagnolli, F.J. Stewart, O. Ulloa, Metaomics unveils the contribution of Alteromonas bacteria to carbon cycling in marine oxygen minimum zones, Front. Mar. Sci. 9 (2022), https://doi.org/10.3389/fmars.2022.993667.

[96] D. De Corte, I. Lekunberri, E. Sintes, G.J. Herndl, Linkage between copepods and bacteria in the north Atlantic Ocean, Aquat. Microb. Ecol. 72 (2014) 215–225, https://doi.org/10.3354/ame01696.

[97] L.M. van der Loos, R. Nijland, Biases in bulk: DNA metabarcoding of marine communities and the methodology involved, Mol. Ecol. 30 (2021) 3270–3288, https://doi.org/10.1111/mec.15592.
[98] G.K. Zhang, F.J.J. Chain, C.L. Abbott, M.E. Cristescu, Metabarcoding using multiplexed markers increases species detection in complex zooplankton communities, Evol Appl 11 (2018) 1901–1914, https://doi.org/10.1111/eva.12694.
[99] S. Peng, W. Hao, Y. Li, L. Wang, T. Sun, J. Zhao, Z. Dong, Bacterial communities associated with four blooming scyphozoan jellyfish: potential species-specific consequences for marine organisms and humans health, Front. Microbiol. 12 (2021), https://doi.org/10.3389/fmicb.2021.647089.
[100] A. Kolda, M. Mucko, A. Rapljenović, Z. Ljubešić, K. Pikelj, Ž. Kwokal, H. Fajković, V. Cuculić, Beach wracks microbiome and its putative function in plastic polluted Mediterranean marine ecosystem, submitted to Marine Environmental Research (2024).
[101] T. Vlachogianni, T. Fortibuoni, F. Ronchi, C. Zeri, C. Mazziotti, P. Tutman, D.B. Varezić, A. Palatinus, Š. Trdan, M. Peterlin, M. Mandić, O. Markovic, M. Prvan, H. Kaberi, M. Prevenios, J. Kolitari, G. Kroqi, M. Fusco, E. Kalampokis, M. Scoullos, Marine litter on the beaches of the Adriatic and Ionian Seas: an assessment of their abundance, composition and sources, Mar. Pollut. Bull. 131 (2018) 745–756, https://doi.org/10.1016/j.marpolbul.2018.05.006.
[102] K. Kesy, M. Labrenz, B.S. Scales, B. Kreikemeyer, S. Oberbeckmann, Vibrio colonization is highly dynamic in early microplastic-associated biofilms as well as on field-collected microplastics, Microorganisms 9 (2021) 76, https://doi.org/10.3390/microorganisms9010076.
[103] A.L. Laverty, S. Primpke, C. Lorenz, G. Gerdts, F.C. Dobbs, Bacterial biofilms colonizing plastics in estuarine waters, with an emphasis on Vibrio spp. and their antibacterial resistance, PLoS One 15 (2020) e0237704, https://doi.org/10.1371/journal.pone.0237704.
[104] M. Miloslavić, D. Lučić, B. Gangai, I. Onofri, Mesh size effects on mesozooplankton community structure in a semi-enclosed coastal area and surrounding sea (South Adriatic Sea), Mar. Ecol. 35 (2014) 445–455, https://doi.org/10.1111/maec.12101.
[105] B. Pestorić, D. Drakulović, D. Lučić, N. Đorđević, D. Joksimović, Zooplankton in Montenegrin adriatic offshore waters, in: A. Joksimović, M. Đurović, I.S. Zonn, A.G. Kostianoy, A.V. Semenov (Eds.), The Montenegrin Adriatic Coast: Marine Biology, Springer International Publishing, Cham, 2021, pp. 107–128, https://doi.org/10.1007/698_2020_703.
[106] F. Kršinić, Vertical distribution of protozoan and microcopepod communities in the South Adriatic Pit, J. Plankton Res. 6 (1998) 1033–1060, https://doi.org/10.1093/plankt/20.6.1033.
[107] Ž. Ninčević Gladan, H. Mihanović, M. Bužančić, O. Vidjak, S. Šestanović, J. Veža, D. Šantić, M. Šolić, B. Grbec, F. Matić, D. Udovičić, H. Prelesnik, Plankton communities in oligotrophic offshore environments in the Eastern Adriatic Sea in relation to mesoscale hydrodynamic fluctuations. https://doi.org/10.2139/ssrn.4551183, 2023.
[108] S. Stefanni, D. Stanković, D. Borme, A. de Olazabal, T. Juretić, A. Pallavicini, V. Tirelli, Multi-marker metabarcoding approach to study mesozooplankton at basin scale, Sci. Rep. 8 (2018) 12085, https://doi.org/10.1038/s41598-018-30157-7.
[109] A. Calbet, F. Carlotti, R. Gaudy, The feeding ecology of the copepod Centropages typicus (Kröyer), Prog. Oceanogr. 72 (2007) 137–150, https://doi.org/10.1016/j.pocean.2007.01.003.
[110] X. He, M. Lei, F. Cheng, S. Hu, In situ food compositions reveal niche partitioning in small marine cladocerans and copepods in Daya Bay, South China Sea, Mar. Ecol. Prog. Ser. 716 (2023) 47–61, https://doi.org/10.3354/meps14363.
[111] J.T. Turner, The feeding ecology of some zooplankters that are important prey items of larval fish. https://www.semanticscholar.org/paper/The-feeding-ecology-of-some-zooplankters-that-are-Turner/c634d4a3fe48b464692dcc8e36c9ec92eab433b5, 1984. (Accessed 3 May 2024).
[112] J.T. Turner, Zooplankton feeding ecology: contents of fecal pellets of the cyclopoid copepods Oncaea venusta, Corycaeus amazonicus, Oithona plumifera, and O. Simplex from the northern gulf of Mexico, Mar. Ecol. 7 (1986) 289–302, https://doi.org/10.1111/j.1439-0485.1986.tb00165.x.